

## COMPLEX DYNAMICS OF A NUTRIENT-PLANKTON SYSTEM WITH NONLINEAR PHYTOPLANKTON MORTALITY AND ALLELOPATHY

ZHIPENG QIU\*

Department of Applied Mathematics  
Nanjing University of Science and Technology  
Nanjing 210094, China

HUAIPING ZHU

Laboratory of Mathematical Parallel Systems (Lamps)  
Department of Mathematics and Statistics  
York University  
Toronto, ON, M3J 1P3, Canada

(Communicated by Sze-Bi Hsu)

**ABSTRACT.** Understanding the plankton dynamics can help us take effective measures to settle the critical issue on how to keep plankton ecosystem balance. In this paper, a nutrient-phytoplankton-zooplankton (NPZ) model is formulated to understand the mechanism of plankton dynamics. To account for the harmful effect of the phytoplankton allelopathy, a prototype for a non-monotone response function is used to model zooplankton grazing, and nonlinear phytoplankton mortality is also included in the NPZ model. Using the model, we will focus on understanding how the phytoplankton allelopathy and nonlinear phytoplankton mortality affect the plankton population dynamics. We first examine the existence of multiple equilibria and provide a detailed classification for the equilibria, then stability and local bifurcation analysis are also studied. Sufficient conditions for Hopf bifurcation and zero-Hopf bifurcation are given respectively. Numerical simulations are finally conducted to confirm and extend the analytic results. Both theoretical and numerical findings imply that the phytoplankton allelopathy and nonlinear phytoplankton mortality may lead to a rich variety of complex dynamics of the nutrient-plankton system. The results of this study suggest that the effects of the phytoplankton allelopathy and nonlinear phytoplankton mortality should receive more attention to understand the plankton dynamics.

**1. Introduction.** Plankton are diverse group of organisms that live in the water column and are incapable of swimming against a current (Lalli and Parsons, 1993). Plankton may be broadly divided into phytoplankton and zooplankton. Phytoplankton are the plants and are mostly unicellular and microscopic in size, and

---

2010 *Mathematics Subject Classification.* Primary: 92D25, 92D40; Secondary: 34A47.

*Key words and phrases.* Nutrient-phytoplankton-zooplankton model, allelopathy, nonlinear phytoplankton mortality, bifurcation, complex dynamics.

This research was partially supported by NSFC grants Nos. 11271190, 11671206 and 11271196 of China and NSERC of Canada.

\* Corresponding author: Zhipeng Qiu.

zooplankton are the heterotrophic plankton which live on phytoplankton. In addition to representing the bottom few levels of a food chain, plankton influence the global carbon cycles, with consequences for climate change that are at present undetermined (Edwards and Brindley, 1999). Although plankton play an important positive role in earth's ecological system, phytoplankton bloom can also bring great harm including disruption of food webs and ecosystem function, contamination of human food supplies and other health effects and poisoning of wildlife and fish (Grover et al., 2012). In recent years, as in other countries around the globe, many of the freshwater lakes in China, especially Taihu, Chaohu and Dianchi are among those which have suffered the algal blooms repeatedly. In Canada, one example is that Lake Erie has been experienced toxic algae blooms since 2003.

The above positive and negative roles that plankton play in the ecological system indicate the importance of keeping plankton ecosystem balance. The issue on how to keep plankton ecosystem balance have received much attention, and great effort has been made towards the understanding of plankton dynamics, recently. Understanding the mechanics of plankton dynamics will help us take effective measures to deal with the important issue. Mathematical modeling of plankton population have provided a useful tool to gain insights into understanding the mechanism.

Since the pioneer work of Riley et al (Riley et al., 1949), many mathematical models have been constructed to describe the dynamical behavior of plankton (Grover et al., 2012; Huppert et al., 2005; Jorgenson, 1976, and references therein). The nutrient-phytoplankton-zooplankton (NPZ) models are important classical models which have been in use in oceanography for at least three decades (Franks, 2002). NPZ models are preliminary approximations, and there is a common bias that the real situation is much more complicated than the 3-compartment NPZ system (Franks, 2002). Yet for the simplicity, the NPZ models allow for theoretical analysis to help us capture the essence of some general feature of the plankton dynamics. Thus, nowadays the NPZ models are still common tools in oceanographic research.

Steele and Henderson (1981) formulated an PZ model to provide an explanations for the differences between enclosures and the open sea; Busenberg et al. (1990) provided a stability analysis for a NPZ model introduced by Wroblewski et al. (1988); Edwards and Brindley (1996, 1999) used the analytical and numerical techniques to study the complex dynamical behavior of two NPZ models; Mukhopadhyay and Bhattacharyya (2006) applied the NPZ model to analyze the role, zooplankton grazing plays, in the determining the dynamics of the NPZ model. These models have provided useful information for understanding the mechanics of plankton dynamics.

Most of these models only assumed that the phytoplankton mortality rate is proportional to the density of phytoplankton (Edwards and Brindley, 1996, 1999; Mukhopadhyay and Bhattacharyya, 2006, and references therein). In fact, intraspecific competition is an inevitable biological phenomena, so the depletion rate of phytoplankton will increase sharply as the density of phytoplankton increases. In order to incorporate intraspecific competition among phytoplankton, in this paper we will assume that the depletion rate of phytoplankton is a quadratic function of phytoplankton in which the linear term represents the phytoplankton mortality rate and the quadratic term represents intraspecific competition among phytoplankton (Freedman and Xu, 1993; Shukla et al., 2008).

Meanwhile, most of the NPZ models also ignored phytoplankton allelopathy. Allelopathy is a biological phenomenon by which an organism produces one or more

biochemicals that influence the growth, survival, and reproduction of other organisms, and has been reported in phytoplankton communities for at least three decades (Roy, 2009). Allelochemicals released by phytoplankton species has both positive and negative effects on the growth of other species (Pal et al., 2009). In recent years, there has been a considerable scientific attention towards the study of allelopathic phytoplankton (Mukhopadhyay et al., 1998; Mukhopadhyay and Bhattacharyya, 2006; Sole et al., 2005, and references therein). In this paper, we will incorporate phytoplankton allelopathy into NPZ models, and assume that phytoplankton allelopathy has negative effects on themselves and zooplankton respectively.

The goal of the paper is to formulate a NPZ model for understanding the effect of the phytoplankton allelopathy and nonlinear phytoplankton mortality due to crowding on the dynamical behavior of nutrient-plankton system. We then studied the mathematical properties of the model both analytically and numerically. It is shown that the system can have up to two positive equilibria. If the system has two positive equilibria, it does not mean that the system has bistability phenomenon which is a common dynamical behavior for many models, especially for some epidemic models (Jiang et al, 2009; Wan and Zhu, 2010) and for a certain parameter region simulation results show that almost solutions of the system are convergent to the boundary equilibrium. Local bifurcation theory is further applied to prove that the system may undergo a Hopf bifurcation which leads to the appearance of limit cycle, and Bogdanov-Takens bifurcation which leads to the existence of both limit cycle and homoclinic orbit. The rich dynamics of the system is also confirmed by numerical simulations. Sufficient conditions for the zero-Hopf bifurcation are also given although we can not provide a numerical example, and numerical results further show that the system may undergo a degenerate Hopf bifurcation but for parameter values not in the biologically meaningful region.

This paper is organized as follows. In Section 2, a simple plankton population (NPZ) model is formulated to simulate the concentration of nutrient, phytoplankton and zooplankton. In Section 3, we will analyze the asymptotical behavior of the NPZ system on the boundary. In Section 4, we will examine the existence of multiple equilibria and provide a detailed classification for the equilibria of the NPZ system. In Section 5, we will analyze the local and global stability of the NPZ system, and local bifurcation theory is further applied to the NPZ system to explore complex dynamics of the system. The paper ends with a discussion and numerical simulations in Section 6.

**2. Model formulation.** In this section, we mainly formulate an NPZ model to describe the changes in the concentrations of nutrient, phytoplankton and zooplankton in a physically homogeneous oceanic mixed layer, and then present some preliminary results.

We use  $N(t)$ ,  $P(t)$  and  $Z(t)$  to represent the instantaneous concentrations of nutrient, phytoplankton, and zooplankton, respectively. Limiting nutrient is assumed to enter reservoir at a rate  $DN_0$ , where  $N_0$  is the input nutrient concentration and  $D$  is the rate of nutrient deliver. The depletion rate of phytoplankton is assumed to be described by the quadratic function  $d_1(P) = d_0 + d_1P$ , where  $d_0$  is the depletion rate of phytoplankton caused by mortality and  $d_1$  is the depletion rate of phytoplankton due to intraspecific competition, and the mortality rate of zooplankton is assumed to be constant  $\delta_2$ . We use the function  $F(N, P)$ ,  $G(P)$  to represent the function of phytoplankton nutrient uptake and the function of zooplankton grazing, respectively;  $\alpha, \beta, 0 < \alpha, \beta < 1$ , represent the phytoplankton growth yield constant and

the zooplankton growth yield constant, and  $\sigma_1$  and  $\sigma_2$  ( $0 < \sigma_1, \sigma_2 < 1$ ) represent nutrient recycling fraction from dead phytoplankton and zooplankton, respectively. With the above assumptions, the system can be described by the following three coupled differential equations:

$$\begin{cases} \frac{dN}{dt} = D(N_0 - N) - F(N, P)P + \sigma_1 d_1(P)P + \sigma_2 d_2(P, Z)Z, \\ \frac{dP}{dt} = \alpha F(N, P)P - G(P)Z - d_1(P)P, \\ \frac{dZ}{dt} = \beta G(P)Z - \delta_2 Z. \end{cases} \quad (1)$$

In order to model the harmful effect of phytoplankton on themselves and zooplankton respectively, in this paper we assume that  $F(N, P)$  is a decreasing function of  $P$  and  $G(P)$  is an inhibition response function of  $P$ . To our knowledge, there are some accepted formulation of the functional form for describing phytoplankton allelopathy (Hsu and Waltman, 2004; Pal et al., 2009), but in this paper we particularly choose the functions  $F(N, P)$  and  $G(P)$  as:

$$F(N, P) = \frac{m_1 N}{1 + k_1 N} \frac{1}{1 + b_1 P};$$

$$G(P) = \frac{m_2 P}{1 + k_2 P} \frac{1}{1 + b_2 P}.$$

In the above equations,  $m_1$  and  $m_2$  are the maximum growth rates of phytoplankton and zooplankton, respectively;  $k_1$  and  $k_2$  are the Michaelis-Menten-Monod constants;  $b_1$  is phytoplankton self-shading coefficient;  $b_2$  is the allelopathic coefficient of phytoplankton.

In view of the above considerations, the system we will investigate is governed by the following specific ordinary differential equations:

$$\begin{cases} \frac{dN}{dt} = D(N_0 - N) - \frac{m_1 N}{1 + k_1 N} \frac{1}{1 + b_1 P} P + \sigma_1 (d_0 + d_1 P)P + \sigma_2 \delta_2 Z, \\ \frac{dP}{dt} = \alpha \frac{m_1 N}{1 + k_1 N} \frac{1}{1 + b_1 P} P - \frac{m_2 P}{1 + k_2 P} \frac{1}{1 + b_2 P} Z - (d_0 + d_1 P)P, \\ \frac{dZ}{dt} = \beta \frac{m_2 P}{1 + k_2 P} \frac{1}{1 + b_2 P} Z - \delta_2 Z, \end{cases} \quad (2)$$

where the definitions of all involving parameters are summarized in Table 1.

The main purpose of the paper is to use (2) to understand how the allelopathic coefficient of phytoplankton  $b_2$  and the depletion rate of phytoplankton due to intraspecific competition  $d_1$  affect the plankton population dynamics. To carry out our analysis, we first discuss the boundedness of the solutions of system (2).

**Theorem 2.1.** *All solutions of system (2) are bounded.*

*Proof.* Let

$$V(N, P, Z) = N(t) + \frac{P(t)}{\alpha} + \frac{Z(t)}{\alpha\beta}.$$

We can see that the function  $V \geq 0$  and  $V \rightarrow +\infty$  when  $N + P + Z \rightarrow +\infty$ . The derivative of  $V$  along the trajectories of system (2) is

$$\frac{dV(t)}{dt}|_{(2)} = D(N_0 - N) - \frac{m_1 N}{1 + k_1 N} \frac{1}{1 + b_1 P} P + \sigma_1 (d_0 + d_1 P)P + \sigma_2 \delta_2 Z$$

TABLE 1. Definitions of frequently used symbols

Parameter	Description
$D$	The washout rate of nutrient
$N_0$	Constant input concentration of nutrient
$\sigma_1$	Nutrient recycling fraction from dead phytoplankton
$\sigma_2$	Nutrient recycling fraction from dead zooplankton
$\alpha$	Phytoplankton growth yield constant
$\beta$	Zooplankton growth yield constant
$m_1$	The maximum growth rate of phytoplankton
$k_1$	The Michaelis-Menten-Monod constant
$b_1$	Plankton self-shading coefficient
$m_2$	The maximum growth rate of zooplankton
$k_2$	The Michaelis-Menten-Monod constant
$d_0$	The depletion rate of phytoplankton caused by mortality
$\delta_2$	The mortality rate of zooplankton
$b_2$	The allelopathic coefficient of phytoplankton
$d_1$	The depletion rate of phytoplankton due to intraspecific competition

$$\begin{aligned}
& + \frac{1}{\alpha} \left( \alpha \frac{m_1 N}{1 + k_1 N} \frac{1}{1 + b_1 P} P - \frac{m_2 P}{1 + k_2 P} \frac{1}{1 + b_2 P} Z - (d_0 + d_1 P) P \right) \\
& + \frac{1}{\alpha \beta} \left( \beta \frac{m_2 P}{1 + k_2 P} \frac{1}{1 + b_2 P} Z - \delta_2 Z \right) \\
& = D(N_0 - N) - \frac{1}{\alpha} (1 - \alpha \sigma_1) \sigma_1 (d_0 + d_1 P) P - \frac{1}{\alpha \beta} (1 - \alpha \beta \sigma_2) \delta_2 Z.
\end{aligned}$$

Since  $0 < \alpha, \beta, \sigma_1, \sigma_2 < 1$ , we can easily see that outside of the region of the positive cone bounded by the three positive coordinate planes and by the surface

$$DN_0 = DN + \frac{1}{\alpha} (1 - \alpha \sigma_1) \sigma_1 (d_0 + d_1 P) P + \frac{1}{\alpha \beta} (1 - \alpha \beta \sigma_2) \delta_2 Z,$$

$\dot{V}(t)$  is negative. According to Yashizawa's theorem (Yoshizawa, 1966), the solutions of system (2) are bounded.  $\square$

**3. Dynamics of the subsystem.** In prepare to analyze the complex dynamics of system (2), we need to obtain the dynamic of system (2) on the boundary without zooplankton. In this case system (2) is reduced to the following NP subsystem:

$$\begin{cases} \frac{dN}{dt} = D(N_0 - N) - \frac{m_1 N}{1 + k_1 N} \frac{1}{1 + b_1 P} P + \sigma_1 (d_0 + d_1 P) P, \\ \frac{dP}{dt} = \alpha \frac{m_1 N}{1 + k_1 N} \frac{1}{1 + b_1 P} P - (d_0 + d_1 P) P. \end{cases} \quad (3)$$

We begin by presenting some notations that will be used in this section. Let

$$\begin{aligned}
\hat{P} &:= \frac{-d_0 + \sqrt{d_0^2 + 4d_1 \frac{D\alpha N_0}{1 - \alpha\sigma_1}}}{2d_1}; \\
f(P) &:= \frac{\alpha m_1 (N_0 - \frac{1 - \alpha\sigma_1}{D\alpha} (d_0 + d_1 P) P)}{1 + k_1 (N_0 - \frac{1 - \alpha\sigma_1}{D\alpha} (d_0 + d_1 P) P)}; \\
g(P) &:= (d_0 + d_1 P)(1 + b_1 P).
\end{aligned}$$

Using the above notations, one can verify through a straightforward computation that

- (1)  $f(0) = \frac{\alpha m_1 N_0}{1 + k_1 N_0}$ ,  $f(\hat{P}) = 0$ ;
- (2)  $f(P) > 0$  and is a decreasing for  $P \in (0, \hat{P})$ .

The subsystem (3) always has the boundary equilibrium  $E_0(N_0, 0)$ . Let  $\mathcal{R}_P$  is the ratio of the phytoplankton's maximum growth rate to its death rate when the subsystem has no phytoplankton, i.e.,

$$\mathcal{R}_P := \frac{\alpha m_1 N_0}{(1 + k_1 N_0)d_0} = \frac{f(0)}{d_0},$$

here  $f(0)$  can be regarded as per capita growth rate. Thus,  $\mathcal{R}_P$  can be explained as the basic reproduction number of the phytoplankton.

**Theorem 3.1.** *If  $\mathcal{R}_P < 1$ , system (3) has only one equilibrium  $E_0(N_0, 0)$  which is globally asymptotically stable; if  $\mathcal{R}_P > 1$ , system (3) has a unstable boundary equilibrium  $E_0(N_0, 0)$  and a locally asymptotically stable positive equilibrium  $E_\partial(N^\partial, P^\partial)$ , where  $P^\partial$  is the unique positive root of the equation  $f(P) = g(P)$  on the interval  $(0, \hat{P})$  and*

$$N^\partial = N_0 - \frac{1 - \alpha\sigma_1}{D\alpha}(d_0 + d_1 P^\partial)P^\partial. \quad (4)$$

*Proof.* The classification for the existence of equilibria is based on a simple algebraic analysis and it is left to the reader. In the following we only consider the stability of the equilibria. Evaluating the Jacobian of subsystem (3) at the boundary equilibrium  $E_0(N_0, 0)$  gives two associated eigenvalues  $\lambda_1 = -D$ ,  $\lambda_2 = f(0) - d_0$ . Thus the equilibrium  $E_0(N_0, 0)$  of subsystem (3) is locally asymptotically stable if  $\mathcal{R}_P < 1$ , and unstable if  $\mathcal{R}_P > 1$ . Since the subsystem (3) has no positive equilibrium if  $\mathcal{R}_P < 1$ , the Pioncare-Bendixson theorem implies that all solutions of subsystem (3) must converge to the equilibrium  $E_0(N_0, 0)$ . Thus the equilibrium  $E_0(N_0, 0)$  of subsystem (3) is globally asymptotically stable if  $\mathcal{R}_P < 1$ .

At the unique positive equilibrium  $E_\partial(N^\partial, P^\partial)$  of subsystem (3), the corresponding characteristic equation is

$$\lambda^2 + A_1(E_\partial)\lambda + A_2(E_\partial) = 0, \quad (5)$$

where

$$\begin{aligned} A_1(E_\partial) &= D + \frac{P^\partial}{1 + b_1 P^\partial} \frac{m_1}{(1 + k_1 N^\partial)^2} + d_0 + 2d_1 P^\partial - \frac{\alpha m_1 N^\partial}{1 + k_1 N^\partial} \frac{1}{(1 + b_1 P^\partial)^2}; \\ A_2(E_\partial) &= D(d_0 + 2d_1 P^\partial - \frac{\alpha m_1 N^\partial}{1 + k_1 N^\partial} \frac{1}{(1 + b_1 P^\partial)^2}) \\ &\quad + (d_0 + 2d_1 P^\partial)(1 - \alpha\sigma_1) \frac{m_1}{(1 + k_1 N^\partial)^2} \frac{P^\partial}{(1 + b_1 P^\partial)^2}. \end{aligned}$$

Noting that

$$d_0 + d_1 P^\partial = \frac{\alpha m_1 N^\partial}{1 + k_1 N^\partial} \frac{1}{1 + b_1 P^\partial} > \frac{\alpha m_1 N^\partial}{1 + k_1 N^\partial} \frac{1}{(1 + b_1 P^\partial)^2},$$

it then follows from the expressions of  $A_1(E_\partial)$  and  $A_2(E_\partial)$  that  $A_1(E_\partial) > 0$ , and  $A_2(E_\partial) > 0$ . These mean that the real part of each root of Eq. (5) is negative, i.e., the positive equilibrium  $E_\partial$  of subsystem (3) is locally asymptotically stable when it exists. This completes the proof of Theorem 3.1  $\square$

**Theorem 3.2.** *If  $\mathcal{R}_P > 1$ , then the positive equilibrium  $E_\partial(N^\partial, P^\partial)$  of subsystem (3) is globally asymptotically stable in  $\mathbb{R}_+^2$ .*

*Proof.* Using the standard method we can prove that if  $\mathcal{R}_P > 1$  the subsystem (3) is uniformly persistent in  $\mathbb{R}_+^2$ . It follows from Theorem 3.1 that the positive equilibrium  $E_\partial(N^\partial, P^\partial)$  of subsystem (3) is locally asymptotically stable if  $\mathcal{R}_P > 1$ . Thus, in order to prove the theorem we only need to prove that subsystem (3) has no periodic orbit in  $\mathbb{R}_+^2$ . Suppose that  $\Gamma(t) = (N(t), P(t))$  is an arbitrary nontrivial periodic orbit of subsystem (3) with the least period  $T > 0$ . Let

$$\begin{aligned}\Delta(\Gamma(t)) &:= \int_0^T \text{Trac}(J(N(t), P(t)))dt \\ &= \int_0^T \left( -D - \frac{P(t)}{1 + b_1 P(t)} \frac{m_1}{(1 + k_1 N(t))^2} + \right. \\ &\quad \left. \frac{\alpha m_1 N(t)}{1 + k_1 N(t)} \frac{1}{(1 + b_1 P(t))^2} - d_0 - 2d_1 P(t) \right) dt,\end{aligned}$$

where  $J(N(t), P(t))$  is the Jacobian matrix of subsystem (3) around the periodic solution  $(N(t), P(t))$ .

Since  $(N(t), P(t))$  is a solution of subsystem (3), it then follows that

$$P'(t) = \frac{\alpha m_1 N(t)}{1 + k_1 N(t)} \frac{1}{1 + b_1 P(t)} P(t) - (d_0 + d_1 P(t))P(t).$$

Rearranging terms, we obtain

$$\frac{\alpha m_1 N(t)}{1 + k_1 N(t)} \frac{1}{(1 + b_1 P(t))^2} = \frac{P'(t)}{P(t)(1 + b_1 P(t))} + \frac{d_0 + d_1 P(t)}{1 + b_1 P(t)}. \quad (6)$$

Substituting Equ. (6) into the expression of  $\Delta(\Gamma(t))$  gives

$$\begin{aligned}\Delta(\Gamma(t)) &:= \int_0^T \frac{P'(t)}{P(t)(1 + b_1 P(t))} dt + \int_0^T \left( -D - d_1 P(t) \right. \\ &\quad \left. - \frac{P(t)}{1 + b_1 P(t)} \frac{m_1}{(1 + k_1 N(t))^2} - \frac{b_1(d_0 + d_1 P(t))P(t)}{1 + b_1 P(t)} \right) dt.\end{aligned}$$

Noting that  $P(t)$  is periodic of period  $T$ , the first integral is equal to zero, and we can easily see that the second integral is negative because the integrand is less than zero for all  $t \in [0, T]$ . It then follows that  $\Delta(\Gamma(t)) < 0$ . Hence, the divergency criterion (Hale, 1980) implies that all the periodic solutions must be orbitally stable. This is impossible, since the unique positive equilibrium  $E_\partial(N^\partial, P^\partial)$  is locally asymptotically stable. Thus, the subsystem (2) has no periodic orbit in  $\mathbb{R}_+^2$ . This completes the proof of Theorem 3.2.  $\square$

It follows from Theorem 3.1 and 3.2 that the dynamics of the subsystem (3) is completely determined by the basic reproduction of the phytoplankton  $\mathcal{R}_P$ . If  $\mathcal{R}_P < 1$ , i.e., the phytoplankton growth rate is less than its death rate Theorem 3.1 implies that the phytoplankton will die out, and if  $\mathcal{R}_P > 1$ , i.e., the phytoplankton growth rate is greater than its death rate Theorem 3.2 implies that the phytoplankton will break out and the concentration of the phytoplankton will eventually tend to the steady state.

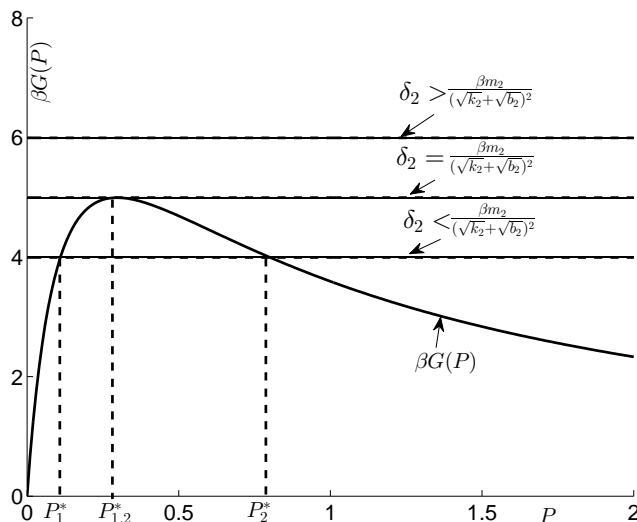


FIGURE 1. The unimodal curve of the function  $\beta G(P)$ . The figure explains the number of positive roots of the equation  $\beta G(P) = \delta_2$ .

4. **Existence and classification of equilibria for the full model.** It follows from the previous section that system (2) has two boundary equilibria  $E_0(N_0, 0, 0)$ ,  $E_\partial(N^\partial, P^\partial, 0)$ . Moreover, the boundary equilibrium  $E_0$  is globally asymptotically stable in the  $N - P$  coordinate plane if  $\mathcal{R}_P < 1$ , and  $E_\partial$  is globally asymptotically stable in the interior of  $N - P$  coordinate plane if  $\mathcal{R}_P > 1$ . In the following, let us discuss the number and classify the positive equilibria of the system (2). Now we define the other two important quantities,  $\mathcal{R}_Z$ ,  $\mathcal{R}_Z$ , as

$$\mathcal{R}_Z := \frac{\beta}{\delta_2} G\left(\frac{1}{\sqrt{k_2 b_2}}\right) = \frac{\beta m_2}{\delta_2 (\sqrt{k_2} + \sqrt{b_2})^2};$$

$$\mathcal{R}_Z := \frac{\beta}{\delta_2} G(P^\partial).$$

One can verify that the function  $G(P) = \frac{m_2 P}{1+k_2 P} \frac{1}{1+b_2 P}$  is increasing on the interval  $(0, \frac{1}{\sqrt{k_2 b_2}})$  and decreasing on the interval  $(\frac{1}{\sqrt{k_2 b_2}}, +\infty)$ , and when  $P = \frac{1}{\sqrt{k_2 b_2}}$  the function  $G(P)$  reaches the maximum  $\frac{\beta m_2}{(\sqrt{k_2} + \sqrt{b_2})^2}$ . From the biological meaning of the parameters,  $G(\frac{1}{\sqrt{k_2 b_2}}) = \frac{\beta m_2}{(\sqrt{k_2} + \sqrt{b_2})^2}$  is the zooplankton maximum growth rate, and  $\mathcal{R}_Z$  is the ratio of the zooplankton growth rate to its death rate. Thus  $\mathcal{R}_Z$  can be explained as the basic reproduction number of the zooplankton. Similarly, when system (2) does not have any zooplankton and is also in balance,  $\mathcal{R}_Z$  can be explained as the invasion reproduction number of the zooplankton.

Now we are able to define the useful parameter  $\lambda$  as follows:

$$\lambda = \begin{cases} \mathcal{R}_P & \text{if } \mathcal{R}_P \leq 1; \\ 1 + \mathcal{R}_Z & \text{if } \mathcal{R}_P > 1, \mathcal{R}_Z \leq 1; \\ 2 + \mathcal{R}_Z & \text{if } \mathcal{R}_P > 1, \mathcal{R}_Z > 1. \end{cases}$$



In the remain part of this section we will use the defined parameter  $\lambda$  to classify the equilibria of system (2). In order to state the results clearly, define lake eutrophication level index

$$\mathcal{R}'_P := \frac{P^\partial}{\frac{1}{\sqrt{k_2 b_2}}} = P^\partial \sqrt{k_2 b_2},$$

and we consider two different environmental cases  $\mathcal{R}'_P > 1$  and  $\mathcal{R}'_P \leq 1$ .

First let us consider the case  $\mathcal{R}'_P > 1$ . The condition  $\mathcal{R}'_P > 1$  implies the phytoplankton concentration is at eutrophication level in the current ecological environment, and it means the increase of the phytoplankton concentration will go against the invasion of zooplankton. In this case we have the following theorem on the classification of equilibria.

**Theorem 4.1.** *Suppose that  $\mathcal{R}'_P > 1$ . Then we have*

1. Assume that  $\lambda \leq 1$ . System (2) has only one boundary equilibrium  $E_0$ .
2. Assume that  $\lambda > 1$ . System (2) has two boundary equilibria  $E_0, E_\partial$ , and can have up to two positive equilibria. More precisely, we have
  - (a): if  $1 < \lambda < 2$ , system (2) has no positive equilibrium;
  - (b): if  $\lambda = 2$ , system (2) has one critical positive equilibrium  $E_{1,2}^*(N_{1,2}^*, P_{1,2}^*, Z_{1,2}^*)$ ;
  - (c): if  $2 < \lambda < 3$ , system (2) two positive equilibria  $E_1^*(N_1^*, P_1^*, Z_1^*)$  and  $E_2^*(N_2^*, P_2^*, Z_2^*)$ ;
  - (d): if  $\lambda \geq 3$ , system (2) has only one positive equilibria  $E_1^*(N_1^*, P_1^*, Z_1^*)$ .

*Proof.* Consider the following algebraic equation

$$\beta G(P) = \frac{\beta m_2 P}{1 + k_2 P} \frac{1}{1 + b_2 P} = \delta_2. \quad (7)$$

On can easily verify that (see Figure 1) if  $\frac{\beta m_2}{(\sqrt{k_2} + \sqrt{b_2})^2} < \delta_2$ , i.e.,  $\mathcal{R}_Z < 1$ , then Equ. (7) has no positive root; if  $\frac{\beta m_2}{(\sqrt{k_2} + \sqrt{b_2})^2} > \delta_2$ , i.e.,  $\mathcal{R}_Z > 1$ , then Equ. (7) has two positive roots  $P_1^* = \frac{\beta m_2 - \delta_2(k_2 + b_2) - \sqrt{\Delta}}{2\delta_2 k_2 b_2}$ ,  $P_2^* = \frac{\beta m_2 - \delta_2(k_2 + b_2) + \sqrt{\Delta}}{2\delta_2 k_2 b_2}$ , where  $\Delta = (\delta_2)^2(k_2 - b_2)^2 + \beta m_2(\beta m_2 - 2\delta_2(k_2 + b_2))$ , and if  $\frac{\beta m_2}{(\sqrt{k_2} + \sqrt{b_2})^2} = \delta_2$ , i.e.,  $\mathcal{R}_Z > 1$ , Equ. (7) has a unique root  $P_{1,2}^* = \frac{1}{\sqrt{k_2 b_2}}$ .

Any positive equilibrium of system (2) must satisfy the following equations:

$$\begin{cases} D(N_0 - N) - \frac{m_1 N}{1 + k_1 N} \frac{1}{1 + b_1 P} P + \sigma_1(d_0 + d_1 P)P + \sigma_2 \delta_2 Z = 0, \\ \alpha \frac{m_1 N}{1 + k_1 N} \frac{1}{1 + b_1 P} P - \frac{m_2 P}{1 + k_2 P} \frac{1}{1 + b_2 P} Z - (d_0 + d_1 P)P = 0, \\ \beta \frac{m_2 P}{1 + k_2 P} \frac{1}{1 + b_2 P} = \delta_2. \end{cases} \quad (8)$$

In the following we only consider case 2(c):  $2 < \lambda < 3$ , and we omit the proofs for the other cases since they can be proved analogically.

Assume that  $2 < \lambda < 3$ . It then follows that  $\mathcal{R}_P > 1, \mathcal{R}_Z > 1$  and  $\mathcal{R}'_Z < 1$ . Because  $\mathcal{R}_P > 1$ , it follows from Theorem 3.1 that system (2) has two boundary equilibria  $E_0, E_\partial$ . In the following we only need to show that system (2) has two positive equilibria if  $2 < \lambda < 3$ .

Since  $\mathcal{R}_Z > 1$ , from the above discussion Equ. (7) has two positive roots  $P_1^*, P_2^*$ . Let  $P^\#$  be  $P_1^*$  or  $P_2^*$ . Substituting the expression of  $P^\#$  into the first and second equations in (8) gives

$$\begin{cases} D(N_0 - N) - \frac{m_1 N}{1 + k_1 N} \frac{1}{1 + b_1 P^\#} P^\# + \sigma_1(d_0 + d_1 P^\#)P^\# + \sigma_2 \delta_2 Z = 0, \\ \alpha \frac{m_1 N}{1 + k_1 N} \frac{1}{1 + b_1 P^\#} P^\# - \frac{m_2 P^\#}{1 + k_2 P^\#} \frac{1}{1 + b_2 P^\#} Z - (d_0 + d_1 P^\#)P^\# = 0. \end{cases} \quad (9)$$

Rearranging and collecting terms, we obtain

$$\begin{cases} Z = \frac{\alpha \beta D}{\delta_2(1 - \alpha \beta \sigma_2)} \left( N_0 - N - \frac{1 - \alpha \sigma_1}{D \alpha} (d_0 + d_1 P^\#)P^\# \right) := \mathcal{F}(N; P^\#), \\ Z = \frac{\beta P^\#}{\delta_2} \left( \frac{m_1 N}{1 + k_1 N} \frac{\alpha}{1 + b_1 P^\#} - (d_0 + d_1 P^\#) \right) := \mathcal{G}(N; P^\#). \end{cases} \quad (10)$$

It then follows that the function  $\mathcal{F}(N; P^\#)$  is an increasing function of  $N$  in the interval  $[0, +\infty)$  and the function  $\mathcal{G}(N; P^\#)$  is a decreasing function of  $N$  in the interval  $[0, +\infty)$ . In the following, we only consider the intersection between the curve  $Z = \mathcal{F}(N; P^\#)$  and the curve  $Z = \mathcal{G}(N; P^\#)$  in the first quadrant.

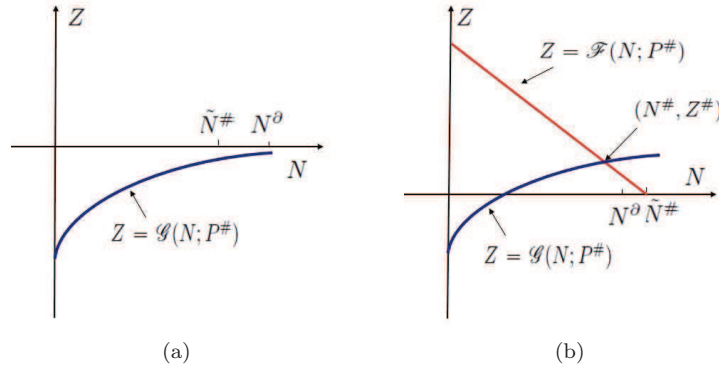


FIGURE 2. The number of positive solutions of Equ. (10) is the same as the number of intersections between the curve  $Z = \mathcal{F}(N; P^\#)$  and the curve  $Z = \mathcal{G}(N; P^\#)$  in the first quadrant. Figure (a) shows that there is no intersection in the first quadrant if  $P^\# \geq P^\partial$ , and Figure (b) shows that there exists a unique intersection in the first quadrant if  $P^\# < P^\partial$ .

Straightforward computation yields that

$$\mathcal{F}(0, P^\#) > 0 > \mathcal{G}(0, P^\#), \mathcal{F}(\tilde{N}^\#; P^\#) = 0,$$

$$\mathcal{G}(\tilde{N}^\#; P^\#) = \frac{\beta P^\#}{\delta_2} \left( f(P^\#) \frac{1}{1 + b_1 P^\#} - (d_0 + d_1 P^\#) \right),$$

where  $\tilde{N}^\# = N_0 - \frac{1 - \alpha \sigma_1}{D \alpha} (d_0 + d_1 P^\#)P^\#$ . If  $P^\# \geq P^\partial$ , then  $N^\partial \leq \tilde{N}^\#$ . Noting that  $\frac{\alpha m_1 N^\partial}{1 + k_1 N^\partial} \frac{1}{1 + b_1 P^\partial} = d_0 + d_1 P^\partial$  and the function  $\mathcal{G}(N; P^\#)$  is a decreasing function of

TABLE 2. Existence of equilibria of system (2).

	$\lambda \leq 1$	$1 < \lambda < 2$	$\lambda = 2$	$2 < \lambda < 3$	$\lambda \geq 3$
$\mathcal{R}'_P > 1$	$E_0$	$E_0, E_\partial$	$E_0, E_\partial, E_{1,2}^*$	$E_0, E_\partial, E_1^*, E_2^*$	$E_0, E_\partial, E_1^*$
$\mathcal{R}'_P \leq 1$	$E_0$	$E_0, E_\partial$		$E_0, E_\partial, E_1^*$	

$N$  in the interval  $[0, +\infty)$ , it then follows that

$$\mathcal{G}(\tilde{N}^\#, P^\#) < \mathcal{G}(N^\partial, P^\#) = \frac{\beta P^\#}{\delta_2} \left( \frac{m_1 N^\partial}{1 + k_1 N^\partial} \frac{\alpha}{1 + b_1 P^\#} - (d_0 + d_1 P^\#) \right) < 0.$$

This implies that the curve  $Z = \mathcal{G}(N; P^\#)$ ,  $0 \leq N \leq N^\#$ , does not pass through the first quadrant (see Figure 2(a)). In this case Equ. (10) does not have a positive solution. If  $P^\# < P^\partial$ , then  $N^\partial > \tilde{N}^\#$ . Similarly, we have

$$\mathcal{G}(\tilde{N}^\#, P^\#) > \mathcal{G}(N^\partial, P^\#) = \frac{\beta P^\#}{\delta_2} \left( \frac{m_1 N^\partial}{1 + k_1 N^\partial} \frac{\alpha}{1 + b_1 P^\#} - (d_0 + d_1 P^\#) \right) > 0.$$

Intermediate Value Theorem implies that there exists a unique interaction between the curve  $Z = \mathcal{F}(N; P^\#)$  and the curve  $Z = \mathcal{G}(N; P^\#)$  in the first quadrant since  $\mathcal{F}(0, P^\#) > 0$ ,  $\mathcal{F}(\tilde{N}^\#, P^\#) = 0$  (see Figure 2(b)). Then Equ. (9) has only one positive solution  $N = N^\#, Z = Z^\#$ . It follows that the positive equilibrium  $E^\#(N^\#, P^\#, Z^\#)$  of system (2) exists if  $\mathcal{R}_Z > 1, P^\# < P^\partial$ .

Since  $\mathcal{R}_Z > 1$ , the conditions  $\mathcal{R}'_Z < 1, \mathcal{R}'_P > 1$ , it then follows that  $P^\partial > P_2^* > P_1^*$ , and from the above discussion the two positive equilibria  $E_1^*(N_1^*, P_1^*, Z_1^*)$ ,  $E_2^*(N_2^*, P_2^*, Z_2^*)$  of system (2) both exist. This completes the proof of Theorem 4.1.  $\square$

Now let us consider the second case that  $\mathcal{R}'_P \leq 1$ . The condition  $\mathcal{R}'_P < 1$  implies the phytoplankton concentration is not at eutrophication level in the current ecological environment, and it means the increase of the phytoplankton concentration will better for the invasion of zooplankton. In the current environmental case, due to the fact that the proof of the corresponding theorem is similar to that of Theorem 4.1 we only state the theorem as follows:

**Theorem 4.2.** Suppose that  $\mathcal{R}'_P \leq 1$ . Then we have

1. Assume that  $\lambda \leq 1$ . System (2) has only one boundary equilibrium  $E_0$ .
2. Assume that  $\lambda > 1$ . System (2) has two boundary equilibria  $E_0, E_\partial$  and no more than one positive equilibrium. More precisely, we have
  - (a): if  $1 < \lambda \leq 2$ , system (2) has no positive equilibrium;
  - (b): if  $\lambda > 2$ , system (2) has only one positive equilibrium  $E_1^*(N_1^*, P_1^*, Z_1^*)$ .

Results stated in Theorem 4.1 and 4.2 are summarized in Table 2.

**5. Stability and bifurcations.** In this section, we mainly investigate the local and global stability of system (2), then apply local bifurcation theory to explore the complex dynamics of system (2). We shall show that system (2) may undergo Hopf, zero-Hopf and Bogdanov-Takens bifurcations. First let us investigate the stability of the boundary equilibria for system (2).

**Theorem 5.1.** 1) The boundary equilibrium  $E_0$  is locally asymptotically stable if  $\lambda < 1$ , and unstable if  $\lambda > 1$ .

2) The boundary equilibrium  $E_\partial$  is locally asymptotically stable if  $1 < \lambda < 3$ , and unstable if  $\lambda > 3$ .

The proof of Theorem 5.1 is similar to that of Theorem 3.1 which lies on lengthy computation of the signs of roots of the characteristic equation, thus we omit it here.

**Theorem 5.2.** *If  $\frac{\alpha m_1}{k_1} < d_0$  or  $\lambda < 1$ ,  $(1 - \alpha\sigma_1)\sigma_1 d_0 > D$ ,  $(1 - \alpha\beta\sigma_2)\sigma_2\delta_2 > D$ , the boundary equilibrium  $E_0$  is globally asymptotically stable.*

*Proof.* From the second equation of system (2), we have

$$\frac{dP}{dt} \leq \left(\frac{\alpha m_1 N}{1 + k_1 N} - d_0\right)P < \left(\frac{\alpha m_1}{k_1} - d_0\right)P. \quad (11)$$

If  $\frac{\alpha m_1}{k_1} < d_0$ , it then follows that  $P(t) \rightarrow 0$  as  $t \rightarrow +\infty$ . From the third equation, we can easily see that  $Z(t) \rightarrow 0$  as  $t \rightarrow +\infty$ . Substituting them into the first equation of (2) yields that  $N(t) \rightarrow N_0$  as  $t \rightarrow +\infty$ , i.e.,  $E_0$  is a global attractor of system (2) if  $\frac{\alpha m_1}{k_1} < d_0$ .

Let  $H(t) = N(t) + \frac{P(t)}{\alpha} + \frac{Z(t)}{\alpha\beta}$ . Then

$$\begin{aligned} \dot{H}(t) &= D(N_0 - N(t)) + \sigma_1(d_0 + d_1 P(t))P(t) + \sigma_2\delta_2 Z - \\ &\quad - \frac{d_0 + d_1 P(t)}{\alpha}P(t) - \frac{\delta_2}{\alpha\beta}Z(t) \\ &\leq DN_0 - DN(t) - \frac{d_0}{\alpha}(1 - \alpha\sigma_1)P(t) - \frac{\delta_2}{\alpha\beta}(1 - \alpha\beta\sigma_2)Z(t). \end{aligned}$$

If  $(1 - \alpha\sigma_1)\sigma_1 d_0 > D$ ,  $(1 - \alpha\beta\sigma_2)\sigma_2\delta_2 > D$  hold, then  $H(t) \leq DN_0 - DH(t)$  which gives that  $H(t) \leq N_0 + H(0)e^{-Dt}$ . Hence,  $\lim_{t \rightarrow +\infty} H(t) = N_0$ , i.e.,

$$\lim_{t \rightarrow +\infty} \left(N(t) + \frac{P(t)}{\alpha} + \frac{Z(t)}{\alpha\beta}\right) = N_0.$$

Since all terms on the left of the above expression are nonnegative, it implies that  $\lim_{t \rightarrow +\infty} N(t) \leq N_0$ . Hence there exists  $T > 0$  such that for  $t > T$ ,  $\alpha \frac{m_1 N(t)}{1 + k_1 N(t)} \frac{P(t)}{1 + b_1 P(t)} \leq f(0)$ . If  $\lambda < 1$ , i.e.,  $\mathcal{R}_P < 1$ , it then follows that  $\dot{P}(t) < 0$  for  $t > T$ , implying that  $\lim_{t \rightarrow +\infty} P(t) = 0$ . From the third equation, we can easily see that  $Z(t) \rightarrow 0$  as  $t \rightarrow +\infty$ . Substituting them into the first equation of (2) yields that  $N(t) \rightarrow N_0$  as  $t \rightarrow +\infty$ , i.e.,  $E_0$  is a global attractor of system (2) if  $\mathcal{R}_P < 1$ ,  $(1 - \alpha\sigma_1)\sigma_1 d_0 > D$ ,  $(1 - \alpha\beta\sigma_2)\sigma_2\delta_2 > D$ . This completes the proof of Theorem 5.1.  $\square$

**Theorem 5.3.** *If  $1 < \lambda < 2$ , the boundary equilibrium  $E_\partial$  of system (2) is globally asymptotically stable.*

*Proof.* From the first result, we only need to prove the boundary equilibrium  $E_\partial$  of system (2) is global attractor. Since the maximum of the function  $\beta G(P)$  is  $\frac{\beta m_2}{(\sqrt{k_2} + \sqrt{b_2})^2}$ , it then follows that

$$\frac{dZ}{dt} = \beta \frac{m_2 P}{1 + k_2 P} \frac{1}{1 + b_2 P} Z - \delta_2 Z \leq \left(\frac{\beta m_2}{(\sqrt{k_2} + \sqrt{b_2})^2} - \delta_2\right)Z. \quad (12)$$

If  $1 < \lambda < 2$ , i.e.,  $\mathcal{R}_P > 1$ ,  $\mathcal{R}_Z < 1$ , we have  $Z(t) \rightarrow 0$  as  $t \rightarrow +\infty$ , and the limiting system of system (2) is subsystem (3). It follows from Theorem 3.2 that if  $\mathcal{R}_P > 1$  the equilibrium  $E_\partial$  is a global attractor of subsystem (3). By using Corollary 4.3

in [31], the boundary equilibrium  $E_\partial$  is also a global attractor of system (2). This completes the proof of Theorem 5.3.  $\square$

Next let us consider the local stability of a positive equilibrium when it exists. Let  $E^\#(N^\#, P^\#, Z^\#)$  be any positive equilibrium of system (2). Linearizing system (2) around the positive equilibrium  $E^\#(N^\#, P^\#, Z^\#)$ , we obtain the matrix

$$J(E^\#) = \begin{pmatrix} -D - \frac{P^\#}{1+b_1P^\#} \times \frac{m_1}{(1+k_1N^\#)^2} & -\frac{m_1N^\#}{1+k_1N^\#} \frac{1}{(1+b_1P^\#)^2} & \sigma_2\delta_2 \\ \frac{\alpha P^\#}{1+b_1P^\#} \frac{m_1}{(1+k_1N^\#)^2} & \frac{\alpha m_1N^\#}{1+k_1N^\#} \frac{1}{(1+b_1P^\#)^2} - (d_0 + 2d_1P^\#) & -\frac{\delta_2}{\beta} \\ 0 & \frac{m_2(1+b_2P^\#) - m_2b_2P^\#(1+k_2P^\#)}{(1+k_2P^\#)^2(1+b_2P^\#)^2} \beta Z^\# & 0 \end{pmatrix}. \quad (13)$$

After extensive algebraic calculations, its characteristic equation is given by

$$\lambda^3 + A_1(E^\#)\lambda^2 + A_2(E^\#)\lambda + A_3(E^\#) = 0, \quad (14)$$

where

$$\begin{aligned} A_1(E^\#) &= D + \frac{P^\#}{1+b_1P^\#} \frac{m_1}{(1+k_1N^\#)^2} - \frac{\alpha m_1N^\#}{1+k_1N^\#} \frac{1}{(1+b_1P^\#)^2} + \\ &\quad \frac{m_2(1+b_2P^\#) - m_2b_2P^\#(1+k_2P^\#)}{(1+k_2P^\#)^2(1+b_2P^\#)^2} Z^\# + (d_0 + 2d_1P^\#); \\ A_2(E^\#) &= (D + \frac{P^\#}{1+b_1P^\#} \frac{m_1}{(1+k_1N^\#)^2})((d_0 + 2d_1P^\#) + \\ &\quad \frac{m_2(1+b_2P^\#) - m_2b_2P^\#(1+k_2P^\#)}{(1+k_2P^\#)^2(1+b_2P^\#)^2} Z^\# - \frac{\alpha m_1N^\#}{1+k_1N^\#} \frac{1}{(1+b_1P^\#)^2}) \\ &\quad + \frac{\delta_2}{\beta} \frac{m_2(1+b_2P^\#) - m_2b_2P^\#(1+k_2P^\#)}{(1+k_2P^\#)^2(1+b_2P^\#)^2} \beta Z^\# + \frac{\alpha P^\#}{1+b_1P^\#} \frac{m_1}{(1+k_1N^\#)^2} \times \\ &\quad (\frac{m_1N^\#}{1+k_1N^\#} \frac{1}{(1+b_1P^\#)^2} - \sigma_1(d_0 + 2d_1P^\#)); \\ A_3(E^\#) &= \frac{m_2(1+b_2P^\#) - m_2b_2P^\#(1+k_2P^\#)}{(1+k_2P^\#)^2(1+b_2P^\#)^2} Z^\# \times \\ &\quad (\delta_2 D + \frac{P^\#}{1+b_1P^\#} \frac{m_1\delta_2}{(1+k_1N^\#)^2} (1 - \alpha\beta\sigma_2)). \end{aligned} \quad (15)$$

Let  $W^u(E^\#)$  be the unstable manifold of  $E^\#$ ,  $W^s(E^\#)$  be its stable manifold and  $W^c(E^\#)$  be its center manifold. Then we have

**Theorem 5.4.** *Let  $E_1^*$  and  $E_2^*$  be the endemic equilibria of system (2) as defined in Theorem 4.1.*

1. *Assume that  $E_1^*$  exists. Then if  $A_1(E_1^*)A_2(E_1^*) - A_3(E_1^*) > 0$ , then  $\dim W^s(E_1^*) = 3$ , i.e.,  $E_1^*$  is locally asymptotically stable; if  $A_1(E_1^*)A_2(E_1^*) - A_3(E_1^*) < 0$ , then  $\dim W^s(E_1^*) = 1$ ,  $\dim W^u(E^\#) = 2$ , i.e.,  $E_1^*$  is unstable, and if  $A_1(E_1^*)A_2(E_1^*) - A_3(E_1^*) = 0$ , then  $\dim W^c(E^\#) = 2$  and  $\dim W^s(E^\#) = 1$ .*
2. *Assume that  $E_2^*$  exists. Then  $E_2^*$  is unstable. More precisely, we have*

- (a): if  $A_1(E_2^*) < 0$ , then  $\dim W^u(E_2^*) = 3, \dim W^s(E_2^*) = 0$  or  $\dim W^u(E_2^*) = 1, \dim W^s(E_2^*) = 2$ ;  
 (b): if  $A_1(E_2^*) \geq 0$ , then  $\dim W^u(E_2^*) = 1, \dim W^s(E_2^*) = 2$ .

*Proof.* We only prove the first case, and the second case can be proved in a similar way. Assume that the equilibrium  $E_1^*(N_1^*, P_1^*, Z_1^*)$  exists, where  $P_1^*$  is a root of (7) and satisfies that

$$\frac{m_2(1 + b_2 P_1^*) - m_2 P_1^*(1 + k_2 P_1^*)}{(1 + k_2 P_1^*)^2 (1 + b_2 P_1^*)^2} > 0.$$

From the second equation of (9), we note that

$$d_0 + d_1 P_1^* > \frac{\alpha m_1 N_1^*}{1 + k_1 N_1^*} \frac{1}{1 + b_1 P_1^*} > \frac{\alpha m_1 N_1^*}{1 + k_1 N_1^*} \frac{1}{(1 + b_1 P_1^*)^2}.$$

It then follows from the expression of  $A_1(E_1^*)$  that  $A_1(E_1^*) > 0$ . Let  $\lambda_1(E_1^*), \lambda_2(E_1^*), \lambda_3(E_1^*)$  be the roots of (14) and, without loss of generality, assume that  $\Re \lambda_1(E_1^*) \leq \Re \lambda_2(E_1^*) \leq \Re \lambda_3(E_1^*)$ . It follows from the relations between the roots and the polynomial coefficients that we have

$$\lambda_1(E^\#) + \lambda_2(E^\#) + \lambda_3(E^\#) = -A_1(E^\#) < 0;$$

$$\lambda_1(E^\#)\lambda_2(E^\#)\lambda_3(E^\#) = -A_3(E^\#) < 0.$$

This means that either  $\lambda_1(E_1^*) < 0 \leq \Re \lambda_2(E_1^*) \leq \Re \lambda_3(E_1^*)$  or  $\Re \lambda_j(E_1^*) < 0$  for all  $j = 1, 2, 3$ .

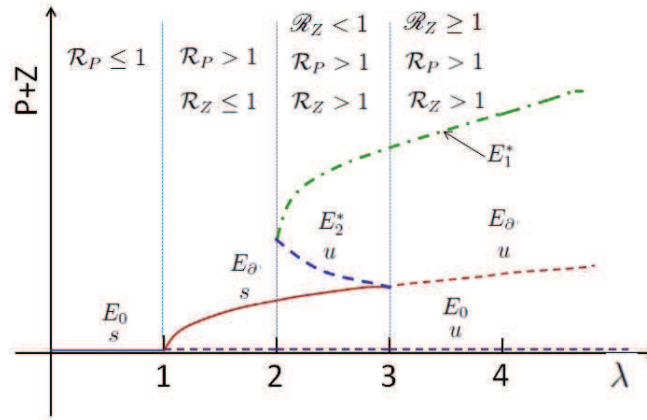
If  $A_1(E_1^*)A_2(E_1^*) - A_3(E_1^*) > 0$ , then the Routh-Hurwitz conditions indicate that  $\Re \lambda_j(E_1^*) < 0$  for  $j = 1, 2, 3$ . By using the Hartman-Grobman Theorem we have  $\dim W^s(E_1^*) = 3$ , i.e.,  $E_1^*$  is locally asymptotically stable. If  $A_1(E_1^*)A_2(E_1^*) - A_3(E_1^*) = 0$  then we have  $A_2(E_1^*) > 0$  since  $A_1(E_1^*) > 0, A_3(E_1^*) > 0$ . It is easy to verify that  $\pm \sqrt{A_2(E_1^*)}i$  are two roots of (14). It also follows from Hartman-Grobman Theorem that  $\dim W^s(E_1^*) = 1, \dim W^c(E_1^*) = 2$ . If  $A_1(E_1^*)A_2(E_1^*) - A_3(E_1^*) < 0$ , then the Routh-Hurwitz conditions indicate that  $\Re \lambda_1(E_1^*) < 0 < \Re \lambda_2(E_1^*) \leq \Re \lambda_3(E_1^*)$ . By using the Hartman-Grobman Theorem we have  $\dim W^s(E_1^*) = 1, \dim W^u(E_1^*) = 2$ . This completes the proof of theorem 5.4.  $\square$

Results stated in Theorem 4.1, 4.2, 5.1, 5.2, 5.3 and 5.4 are also summarized in the bifurcations diagrams shown in Figure 3. Figure 3(a) describes the dynamics of system (2) for the case that  $\mathcal{R}'_P > 1$  and Figure 3(b) shows the dynamics of system (2) for the case that  $\mathcal{R}'_P \leq 1$ . From Figure 3(a), we observe that there is a backward bifurcation for  $\mathcal{R}'_P > 1$ , i.e., multiple positive equilibria exist when the zooplankton invasion reproductive number  $\mathcal{R}'_Z$  is less than unity. Theorem 5.4 further shows that the positive equilibrium  $E_1^*$  is locally asymptotically stable if  $A_1(E_1^*)A_2(E_1^*) - A_3(E_1^*) > 0$ , and unstable if  $A_1(E_1^*)A_2(E_1^*) - A_3(E_1^*) < 0$ . Next, we show that as the positive equilibrium  $E_1^*$  loses its stability, periodic solutions can bifurcate from the positive equilibrium  $E_1^*$ .

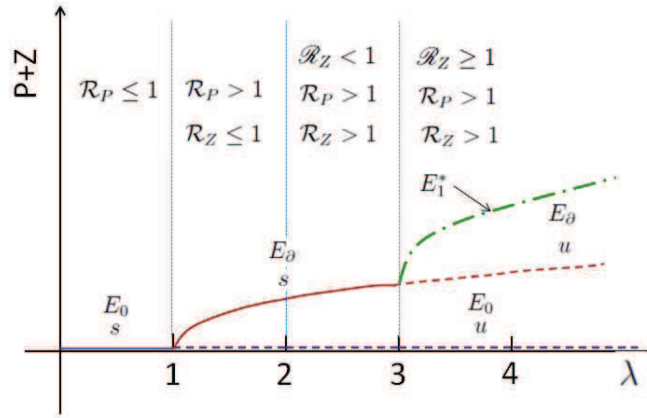
We choose  $b_2$  (the allelopathic coefficient of phytoplankton) to be the bifurcation parameter. For simplicity, we introduce new notions. Let  $E_1^*$  be the corresponding positive equilibrium of system (2), and rewrite the characteristic equation (14) as

$$\lambda^3 + A_1(b_2)\lambda^2 + A_2(b_2)\lambda + A_3(b_2) = 0.$$

We can establish the following theorem.



(a)



(b)

FIGURE 3. Bifurcation diagram for system (2). Solid lines denote stable equilibria (s), dashed lines denote unstable equilibria (u): (a) the case  $\mathcal{R}'_p > 1$ ; (b) the case  $\mathcal{R}'_p \leq 1$ .

**Theorem 5.5.** Assume that the positive equilibrium  $E_1^*$  of system (2) exists, and set

$$\mathcal{H}(b_2) = A_1(b_2)A_2(b_2) - A_3(b_2).$$

If there exists  $b_2 = b_2^c$  such that

$$\mathcal{H}(b_2^c) = 0, \mathcal{H}'(b_2^c) < 0 (\mathcal{H}'(b_2^c) > 0), \quad (16)$$

then the endemic equilibrium  $E_1^*$  is locally stable (unstable) if  $b_2 < b_2^c$  and  $b_2^c - b_2 \ll 1$ , while it is unstable (locally stable) for  $b_2 > b_2^c$  and  $b_2 - b_2^c \ll 1$ , and a Hopf bifurcation occurs at  $b_2 = b_2^c$ .

*Proof.* We only prove the conclusion outside the brackets. The conclusion inside the brackets can be proved in a similar way. The fact that  $\mathcal{H}'(b_2^c) < 0$  indicates that  $\mathcal{H}(b_2)$  is a monotonic decreasing function in the neighborhood of  $b_2 = b_2^c$ . This, together with  $\mathcal{H}(b_2^c) = 0$ , implies that  $\mathcal{H}(b_2) > 0$  for  $b_2 < b_2^c$  and  $b_2^c - b_2 \ll 1$ .

Thus, by Theorem 5.4 we have  $\Re \lambda_j(E_1^*) < 0$  for  $j = 1, 2, 3$  since  $A_1(b_2^c) > 0$ . Thus the positive equilibrium  $E_1^*(N_1^*, P_1^*, Z_1^*)$  is locally stable. The fact that  $\mathcal{H}(b_2^c)$  is a monotonic decreasing function in the neighborhood  $b_2 = b_2^c$  also implies that  $\mathcal{H}(b_2) < 0$  for  $b_2 > b_2^c$  and  $b_2 - b_2^c \ll 1$ . Then, it follows from Theorem 5.4 that we have  $\lambda_1(E_1^*) < 0$  and  $\Re \lambda_2(E_1^*) > 0, \Re \lambda_3(E_1^*) > 0$  since  $A_1(b_2^c) > 0$ , which implies that the positive equilibrium  $E_1^*$  is unstable. According to the result in Liu (1994), the conditions  $\mathcal{H}(b_2^c) = 0$  and  $\mathcal{H}'(b_2^c) < 0$  imply the occurrence of a simple Hopf bifurcation at  $b_2 = b_2^c$ .  $\square$

Now we consider the case when the two positive equilibria  $E_1^*, E_2^*$  coalesce. It follows from Theorem (4.1) that when  $\mathcal{R}'_P > 1, \lambda = 2$  hold the two positive equilibria  $E_1^*, E_2^*$  coalesce into the unique positive equilibrium  $E_{1,2}^*$ . Next we will show that system (2) may undergo zero-Hopf bifurcation and Bogdanov-Takens bifurcation. Because the two bifurcations are at least of codim 2, we choose  $b_2, d_1$  to be the bifurcation parameters, and denote the equilibrium  $E_{1,2}^*$  by  $E_{1,2}^*(N_{1,2}^*(b_2, d_1), P_{1,2}^*(b_2, d_1), Z_{1,2}^*(b_2, d_1))$ . The characteristic equation (14) can be simplified to

$$\lambda^3 + A_1(b_2, d_1)\lambda^2 + A_2(b_2, d_1)\lambda + A_3(b_2, d_1) = 0. \quad (17)$$

where  $A_1(b_2, d_1), A_2(b_2, d_1), A_3(b_2, d_1)$  are defined in (15). Then we have the following results:

**Theorem 5.6.** *If there exists  $d_1 = d_1^z, b_2 = b_2^z$  such that*

$$1) \mathcal{R}'_P(b_2^z, d_1^z) > 1, \lambda(b_2^z, d_1^z) = 2;$$

$$2) A_1(b_2^z, d_1^z) = 0, A_2(b_2^z, d_1^z) > 0, \frac{\partial A_1}{\partial b_2}|_{(b_2^z, d_1^z)} A_2(b_2^z, d_1^z) - \frac{\partial A_3}{\partial b_2}|_{(b_2^z, d_1^z)} \neq 0,$$

*then a zero-Hopf bifurcation occurs at  $b_2 = b_2^z, d_1 = d_1^z$ .*

*Proof.* Since there exists  $d_1 = d_1^z, b_2 = b_2^z$  such that  $\mathcal{R}'_P(d_1^z, b_2^z) > 1, \lambda(d_1^z, b_2^z) = 2$ , it then follows from Theorem 4.1 that system (2) has only one positive equilibrium  $E_{1,2}^*(N_{1,2}^*(b_2^z, d_1^z), P_{1,2}^*(b_2^z, d_1^z), Z_{1,2}^*(b_2^z, d_1^z))$ . Straightforward computation yields that the characteristic equation associated with system (2) around the equilibrium  $E_{1,2}^*$  can be expressed as

$$\lambda^3 + A_1(b_2^z, d_1^z)\lambda^2 + A_2(b_2^z, d_1^z)\lambda + A_3(b_2^z, d_1^z) = 0, \quad (18)$$

where  $A_3(b_2^z, d_1^z) = 0$ . The conditions  $A_1(b_2^z, d_1^z) = 0, A_2(b_2^z, d_1^z) > 0$  imply that the characteristic roots of the equation (18) are  $\lambda_1 = 0, \lambda_2 = i\sqrt{A_2(b_2^z, d_1^z)}, \lambda_3 = -i\sqrt{A_2(b_2^z, d_1^z)}$ , respectively, i.e., system (2) has the positive equilibrium  $E_{1,2}^*$  with one zero eigenvalue and a pair of purely imaginary eigenvalues.

Since the function  $\frac{m_2 P}{(1+k_2 P)(1+b_2 P)}$  is a decreasing function of  $b_2$ , we can easily see that the third equation of (8) has two roots if  $b_2 < b_2^z$  and no root if  $b_2 > b_2^z$ . Using the same way as in the discussion in Theorem 4.1 it follows that for any given  $d_1, 0 \leq |d_1 - d_1^z| \ll 1$  system (2) has two positive equilibria if  $b_2 < b_2^z$  and no positive equilibrium if  $b_2 > b_2^z$ . Thus, the line

$$T = \{(b_2, d_1) | b_2 = b_2^z, |d_1 - d_1^z| \ll 1\}$$

corresponding to a fold bifurcation: along this curve system (2) has an equilibrium with a zero eigenvalue. If  $d_1 \neq d_1^z$ , then the fold bifurcation is nondegenerate and crossing  $T$  from right to left implies the appearance of two positive equilibria. Thus saddle-node bifurcation occurs at the point  $b_2 = b_2^z, d_1 = d_1^z$ .



Now let us determine the sign of the derivative of  $\Re \lambda_2(b_2, d_1)$  at the point  $b_2 = b_2^z, d_1 = d_1^z$ . From the characteristic equation (17), we have

$$(3\lambda^2 + 2A_1(b_2, d_1)\lambda + A_2(b_2, d_1)) \frac{\partial \lambda(b_2, d_1)}{\partial b_2} = -\left(\frac{\partial A_1(b_2, d_1)}{\partial b_2} \lambda^2 + \frac{\partial A_2(b_2, d_1)}{\partial b_2} \lambda + \frac{\partial A_3(b_2, d_1)}{\partial b_2}\right).$$

Thus,

$$\frac{\partial \lambda(b_2, d_1)}{\partial b_2} = -\frac{\frac{\partial A_1(b_2, d_1)}{\partial b_2} \lambda^2 + \frac{\partial A_2(b_2, d_1)}{\partial b_2} \lambda + \frac{\partial A_3(b_2, d_1)}{\partial b_2}}{3\lambda^2 + 2A_1(b_2, d_1)\lambda + A_2(b_2, d_1)}.$$

Hence,

$$\begin{aligned} & \text{Sign}\left\{\frac{\partial \Re \lambda(b_2, d_1)}{\partial b_2}\right\}_{\lambda=i\sqrt{A_2(b_2^z, d_1^z)}} = \text{Sign}\left\{\Re\left(\frac{\partial \lambda(b_2, d_1)}{\partial b_2}\right)\right\}_{\lambda=i\sqrt{A_2(b_2^z, d_1^z)}} \\ &= \text{Sign}\left\{\Re\left[-\frac{\frac{\partial A_1(b_2, d_1)}{\partial b_2} \lambda^2 + \frac{\partial A_2(b_2, d_1)}{\partial b_2} \lambda + \frac{\partial A_3(b_2, d_1)}{\partial b_2}}{3\lambda^2 + 2A_1(b_2, d_1)\lambda + A_2(b_2, d_1)}\right]_{\lambda=i\sqrt{A_2(b_2^z, d_1^z)}}\right\} \\ &= \text{Sign}\left\{\Re\left[-\frac{\frac{\partial A_1(b_2, d_1)}{\partial b_2} \lambda^2 + \frac{\partial A_2(b_2, d_1)}{\partial b_2} \lambda + \frac{\partial A_3(b_2, d_1)}{\partial b_2}}{3\lambda^2 + 2A_1(b_2, d_1)\lambda + A_2(b_2, d_1)}\right]_{\lambda=i\sqrt{A_2(b_2^z, d_1^z)}}\right\} \\ &= \text{Sign}\left\{\frac{\frac{\partial A_3}{\partial b_2}|_{(d_2^z, d_1^z)}}{2A_2(b_2^z, d_1^z)} - \frac{\frac{\partial A_1}{\partial b_2}|_{(b_2^z, d_1^z)} A_2(b_2^z, d_1^z)}{2A_2(b_2^z, d_1^z)}\right\} \end{aligned}$$

The condition  $A_1(b_2^z, d_1^z)$  was used in the last step. The assumptions  $A_2(b_2^z, d_1^z) > 0$  and  $\frac{\partial A_1}{\partial b_2}|_{(b_2^z, d_1^z)} A_2(b_2^z, d_1^z) - \frac{\partial A_3}{\partial b_2}|_{(b_2^z, d_1^z)} \neq 0$  imply that

$$\text{Sign}\left\{\frac{\partial \Re \lambda(b_2, d_1)}{\partial b_2}\right\}_{\lambda=i\sqrt{A_2(b_2^z, d_1^z)}} \neq 0.$$

Thus we can see that at  $b_2 = b_2^z, d_1 = d_1^z$  the pair  $(\lambda_2, \lambda_3)$  of complex conjugate eigenvalues crosses the imaginary axis with non-zero speed “from the right to the left”. Then it follows from Theorem 1.2 of Hassard et al. (1981) that a Hopf bifurcation occurs at  $b_2 = b_2^z, d_1 = d_1^z$ . From the above discussion, system (2) can undergo the saddle node bifurcation and Hopf bifurcation at the point  $b_2 = b_2^z, d_1 = d_1^z$ , thus if occurs, the zero-Hopf bifurcation occurs at the  $b_2 = b_2^z, d_1 = d_1^z$ . This completes the proof of Theorem 5.6.  $\square$

Using the similar way as in the proof of Theorem 5.6, we obtain that  $A_3(b_2^b, d_1^b) = 0$  if the assumptions  $\mathcal{R}'_P(b_2^z, d_1^z) > 1, \lambda(b_2^z, d_1^z) = 2$  hold, where  $A_3(b_2^b, d_1^b)$  is defined in (15). This, together with the assumptions that  $A_2(b_2^b, d_1^b) = 0, A_1(b_2^b, d_1^b) \neq 0$ , implies that the characteristic roots of the equation (18) are  $\lambda_1 = 0, \lambda_2 = 0, \lambda_3 \neq 0$ , respectively, i.e., system (2) has the positive equilibrium  $E_{1,2}^*(N_{1,2}^*(b_2^z, d_1^z), P_{1,2}^*(b_2^z, d_1^z), Z_{1,2}^*(b_2^z, d_1^z))$  with two zero eigenvalues and a nonzero eigenvalue. A straightforward computation yields that

$$\begin{vmatrix} -D - \frac{P_{1,2}^*}{1+b_1 P_{1,2}^*} & \sigma_2 \delta_2 \\ \times \frac{m_1}{(1+k_1 N_{1,2}^*)^2} & \\ \frac{\alpha P_{1,2}^*}{1+b_1 P_{1,2}^*} \frac{m_1}{(1+k_1 N_{1,2}^*)^2} & -\frac{\delta_2}{\beta} \end{vmatrix} = \frac{D\delta_2}{\beta} + \frac{\delta_2}{\beta} \frac{P_{1,2}^*}{1+b_1 P_{1,2}^*} \frac{m_1}{(1+k_1 N_{1,2}^*)^2} (1 - \alpha\beta\sigma_2) > 0$$

since  $0 < \sigma_2, \alpha, \beta < 1$ . It then follows that  $\text{Rank}(J(E_{1,2}^*)) = 2$  and the Jordan

normal form of Jacobian matrix  $J(E_{1,2}^*)$  must be the following form  $\begin{pmatrix} * & 0 & 0 \\ 0 & 0 & 1 \\ 0 & 0 & 0 \end{pmatrix}$ ,

where  $*$  represents a non-zero real number. From the above discussion, we can see that, at  $b_2 = b_2^b, d_1 = d_1^b$ , system (2) has the equilibrium  $E_{1,2}^*$  with a nonzero eigenvalue, two zero eigenvalues and the zero Jordan block of order 2. Thus it follows from the theory of Bogdanov-Takens bifurcation (Kuznetsov, 1998) that the Bogdanov-Takens bifurcation possibly occurs at  $b_2 = b_2^b, d_1 = d_1^b$ . Thus we have the following conclusion.

**Conclusion:** If there exists  $b_2 = b_2^b, d_1 = d_1^b$  such that

$$1) \mathcal{R}'_P(b_2^b, d_1^b) > 1, \lambda(b_2^b, d_1^b) = 2;$$

$$2) A_2(b_2^b, d_1^b) = 0, A_1(b_2^b, d_1^b) \neq 0,$$

then a Bogdanov-Takens bifurcation possibly occurs at  $b_2 = b_2^b, d_1 = d_1^b$ .

**6. Simulations and discussion.** In this section, we mainly summarize our results and present numerical simulations for system (2). These simulations not only confirm the analytical results described in the previous section, but also extend these results to more general case and illustrate more complex behaviors of system (2).

In this paper, we proposed an NPZ mathematical model to understand the mechanics of plankton dynamics, and two important factors, nonlinear phytoplankton mortality and phytoplankton allelopathy, are both incorporated into the NPZ model. In order to investigate the dynamics of the NPZ model, we define four indexes which are the lake eutrophication level index  $\mathcal{R}_P$  and three reproduction number indexes  $\mathcal{R}_P, \mathcal{R}_Z, \mathcal{R}_Z$ , and using the three reproduction number indexes we further define an important index  $\lambda$ . Then the two parameters  $\lambda, \mathcal{R}'_P$  are used to classify the existence and stability of the equilibria for the full NPZ model. We are sure that the unique boundary equilibrium  $E_0$  is globally asymptotically stable if  $\lambda \leq 1$  and the boundary equilibrium  $E_\partial$  is globally asymptotically stable in the case that  $\mathcal{R}'_P > 1, 1 < \lambda < 2$  or  $\mathcal{R}'_P \leq 1, 1 < \lambda < 3$ , although in this paper we only provided sufficient conditions for the global stability. Using a similar argument as in the proof of Theorem 2.3 of Wang and Zhao (2004), we can rigorously prove that the full NPZ system (2) is uniformly persistent if  $\lambda > 3$ , i.e., the phytoplankton and zooplankton can coexist in the current environment. The above theoretical results indicate that the dynamics of the full NPZ system can be almost determined by the indexes. For each given lake, its related parameters decide or characterize the basic feature of the ecosystem. Thus, with the lake eutrophication level index  $\mathcal{R}'_P$  and three reproduction number indexes  $\mathcal{R}_P, \mathcal{R}_Z, \mathcal{R}_Z$ , i.e.,  $\lambda$ , we can roughly categorize the lakes based on their features.

Subsequently, bifurcation theory are applied to investigate the local bifurcation of the full NPZ system by choosing  $b_2$  and  $d_1$  as bifurcation parameters. The theoretical results suggest that the phytoplankton allelopathy and nonlinear phytoplankton mortality may lead to a rich variety of dynamics of the nutrient-plankton system. These theoretical results are also confirmed/extended by the following simulation results. In the numerical studies the parameters for allelopathic coefficient of phytoplankton  $b_2$  and the depletion rate of phytoplankton due to intraspecific competition  $d_1$  are chosen to vary, and the other parameter values are supposedly fixed. The other parameter values used in the simulation are given as follows:

$$D = 0.1, N_0 = 200, k_1 = 2, m_1 = 10, b_1 = 2, \sigma_1 = 0.825,$$

$$d_0 = 1.4, \alpha = 0.8, \beta = 0.6, m_2 = 120, k_2 = 2, \sigma_2 = 0.6, \delta = 5.$$

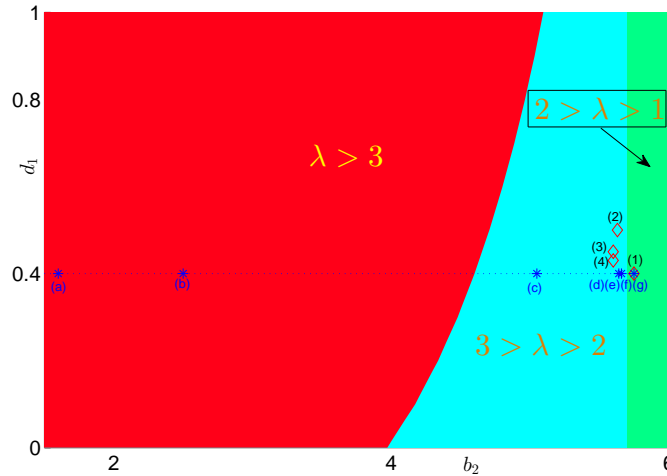


FIGURE 4. A bifurcation diagram for  $\lambda$  in the  $(b_2, d_1)$ -plane. In the red region the corresponding  $\lambda$  values are greater than 3, in blue region the corresponding  $\lambda$  values are between 2 and 3, and in green region the corresponding  $\lambda$  values are between 1 and 2. Various  $(b_2, d_1)$  values denoted by  $\diamond$  and  $*$  are used in Figure 6 and 9, respectively, to numerically simulate the dynamics of system (2).

Using the parameter values listed above, straightforward computation yields that  $\mathcal{R}'_P > 1$  if  $b_2 > 0.05$  or  $d_1 > 0.04$ . In the following we only consider the case that  $\mathcal{R}'_P > 1$ . Figure 4 shows a bifurcation diagram for  $\lambda$  in the  $(b_2, d_1)$ -plane. In Figure 4, if  $(b_2, d_1)$  lies in the red region, then the corresponding  $\lambda$  value is greater than 3; if  $(b_2, d_1)$  lies in the blue region, then the corresponding  $\lambda$  value is greater than 2 and less than 3, and if  $(b_2, d_1)$  lies in the green region, then the corresponding  $\lambda$  value is greater than 1 and less than 2. It then follows from the previous discussion that the dynamics of the full NPZ model is roughly determined by the two curves  $\lambda(b_2, d_1) = 2$  and  $\lambda(b_2, d_1) = 3$ . For example, if the value of  $(b_2, d_1)$  lies in the red region, i.e.,  $\lambda > 3$ , the zooplankton and phytoplankton will coexist, and if the value of  $(b_2, d_1)$  lies in the green region, i.e.,  $1 < \lambda < 2$ , then the zooplankton and phytoplankton will both die out.

By using the `matcont`, we also generate fold and Hopf curves in the  $(b_2, d_1)$ -plane as show in Figure 5. The existence of positive equilibria of system (2) is determined by the fold curve. If the point  $(b_2, d_1)$  lies in the right side of fold curve, system (2) has no positive equilibrium; if the point  $(b_2, d_1)$  lies in the left side of fold curve, then system (2) has at least one positive equilibrium, in particularly, system (2) has two positive equilibria if the point  $(b_2, d_1)$  is sufficiently close to fold curve from the left. The point denoted by BT separates the fold curve into two branches denoted by  $T_+$ ,  $T_-$  respectively. Through simulations we can check that passage through  $T_-$  implies the coalescence of a stable nodes  $E_1^*$  and a saddle point  $E_2^*$ , while crossing  $T_+$  generates an unstable node  $E_1^*$  and a saddle point  $E_2^*$ .

The Hopf bifurcation curve is a curve on which the equilibrium  $E_1^*$  has a pair of eigenvalues with zero sum:  $\lambda_1 + \lambda_2 = 0$ . The part of Hopf curve denoted by full

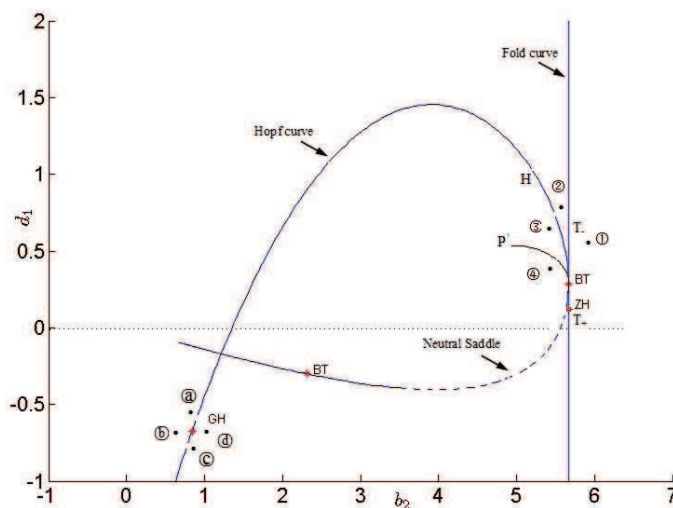


FIGURE 5. Fold and Hopf curves in NPZ model: BT-Bogdanov-Takens, GH-generalized Hopf points.

line corresponds to a nondegenerate Hopf bifurcation ( $\lambda_{1,2} = \pm i\omega$ ) while the part of Hopf curve denoted by dotted line is not a nonbifurcation line corresponding to a neutral saddle. Simulation results also show that the first Lyapunov coefficient  $l_1 < 0$  if the point  $(b_2, d_1)$  is on the Hopf curve denoted by full line and  $d_1 > 0$ . This means that Hopf bifurcation gives rise to a stable limit cycle.

From Figure 5, we observe that the fold curve and Hopf curve are tangent at a point  $b_2 = 5.667, d_1 = 0.2827$  denoted by BT. This implies that system (2) exhibits Bogdanov-Takens bifurcation at the point  $b_2 = 5.667, d_1 = 0.2827$ . The two curves separates the  $b_2$ - $d_1$  plane into three regions. In order to obtain more detailed information on the Bogdanov-Takens bifurcation, various values of  $b_2, d_1$  are chosen in different regions according to the bifurcation diagram in Figure 5, and then by using these given parameter values we simulate the dynamical behavior of system (2). These behaviors are illustrated in Figure 6. These values of  $(b_2, d_1)$  are  $(5.70, 0.40), (5.63, 0.5), (5.60, 0.45), (5.60, 0.43)$  in Figures 6(a), (b), (c) and (d), respectively, and the  $(b_2, d_1)$  values are denoted by  $\diamond$  in Figure 4 from which we can obtain the corresponding  $\lambda$  values.. In Figure 6(a), the point  $(b_2, d_1) = (5.667, 0.2827)$  lies in the right side of fold curve. In this case, it follows from the theoretical results that system (2) has no positive equilibrium, and all solutions are convergent to the boundary equilibrium  $E_{\partial}$ ; In Figure 6(b), it shows that there are two positive equilibria, and we observe that, depending on initial conditions, solutions may either converge to the positive equilibrium  $E_1^*$  or converge to the boundary equilibrium  $E_{\partial}$ . In Figure 6(c), we observe a stable periodic solutions. Again, depending on initial conditions, solutions may either converge to the periodic solution or converge to the boundary equilibrium  $E_{\partial}$ . In Figure 6(d), although the two positive equilibria are both unstable, there is no stable periodic solution. It shows that all solutions converge to the boundary equilibrium. Based on the theory of the Bogdanov-Takens bifurcation (Kuznetsov, 1998), it then follows that there is a limit cycle bifurcation curve P emanating from the BT point, along which there is a homoclinic orbit to the saddle  $E_2^*$ .

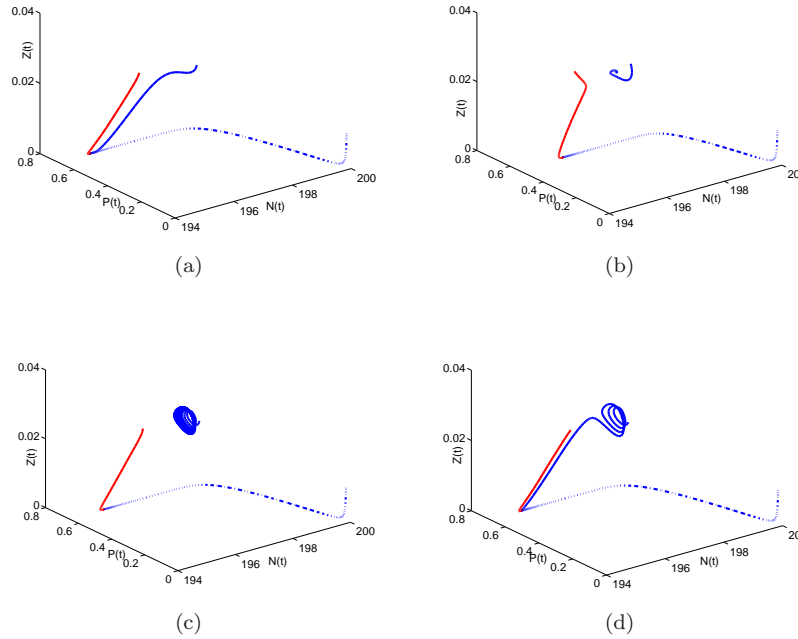


FIGURE 6. Numerical simulations of system (2) for various  $(b_2, d_1)$  values chosen according to the bifurcation diagram in Figure 5: (a)  $(b_2, d_1) = (5.70, 0.40)$ ; (b)  $(b_2, d_1) = (5.63, 0.50)$ ; (c)  $(b_2, d_1) = (5.63, 0.45)$ , and (d)  $(b_2, d_1) = (5.63, 0.43)$

The Hopf bifurcation can be degenerate if first Lyapunov coefficient vanishes. Along the Hopf bifurcation curve, we observe that the first Lyapunov coefficient vanishes at the point  $(b_2, d_1) = (0.8414, -0.6727)$  denoted by GH. This implies that system (2) exhibits generalized-Hopf bifurcation at GH. Yet, the parameter values are not in the biologically meaningful region. According to the bifurcation diagram in Figure 5, various values of  $b_2, d_1$  are also chosen in different region to simulate the dynamical behavior of system (2). These dynamical behaviors are illustrated in Figure 7. The parameter values of  $(b_2, d_1)$  used in Figures 7(a), (b), (c), (d) are  $(0.8414, -0.6527)$ ,  $(0.8214, -0.6727)$ ,  $(0.8414, -0.6927)$ ,  $(0.8614, -0.6727)$ , respectively. From these figures, we also observe that the parameters  $b_2$  and  $d_1$  may cause the nutrient-plankton system a rich variety of dynamics, such as multiple stable periodic solutions, quasi-periodic solution.

Next, we present some numerical results on how the change in  $b_2$  (the allelopathic coefficient of phytoplankton) may affect the dynamical behavior of system (2). Figure 8 shows a bifurcation diagram for the system (2), with  $b_2$  as the bifurcation parameter and a fixed value of  $d_1 = 0.4$ . All other parameter values are the same as those in Figure 5. In this case, a positive equilibrium exists only for  $b_2 < b_2^{LP} \approx 5.667$  (here LP denote limit point), and there are two branches of positive equilibria, with the top and bottom branches corresponding to  $E_1^*$  and  $E_2^*$ , respectively. Denote  $E_i^* = E_i^*(b_2), i = 1, 2$ . From Figure 8 we can easily see that  $E_2^*(b_2)$  exists only for  $b_2^{BP} < b_2 < b_2^{LP}$ , where  $b_2^{BP} \approx 4.601$ , and it

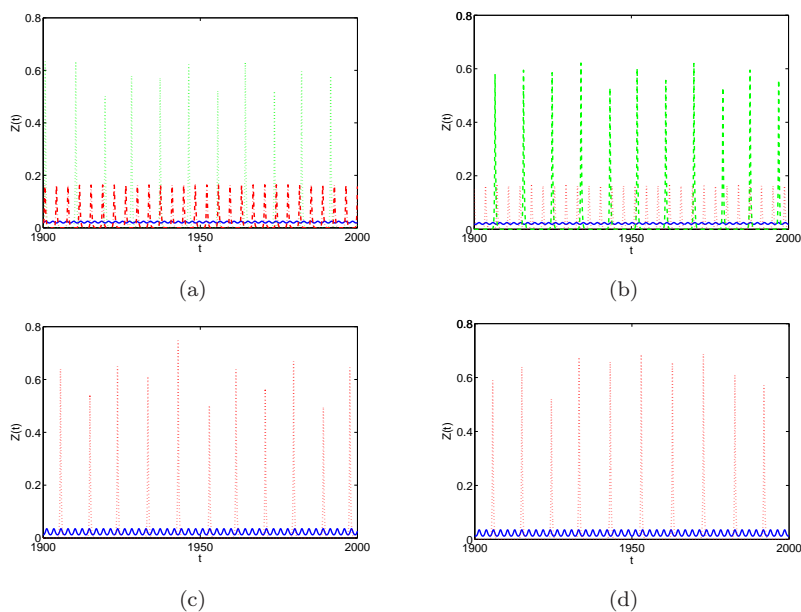


FIGURE 7. Numerical simulations of system (2) for various  $(b_2, d_1)$  values chosen according to the bifurcation diagram in Figure 5: (a)  $(b_2, d_1) = (0.8414, -0.6527)$ ; (b)  $(b_2, d_1) = (0.8214, -0.6727)$ ; (c)  $(b_2, d_1) = (0.8414, -0.6927)$ , and (d)  $(b_2, d_1) = (0.8614, -0.6727)$ .

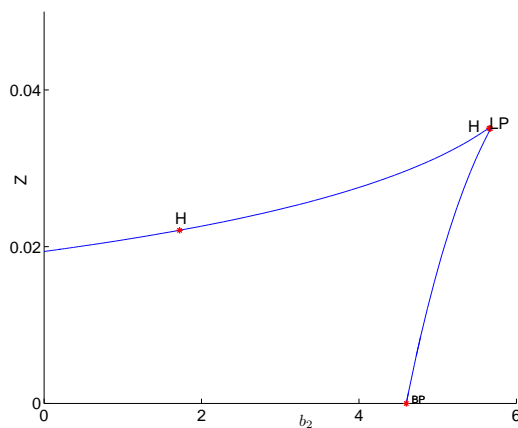


FIGURE 8. Plot of the positive equilibria versus  $b_2$  for system (2). The value of  $d_1$  is chosen to be  $d_1 = 0.4$ . It shows that there are two branches of positive equilibria, separated by a limit point (LP). The top branch corresponds to  $E_1^*$  and the bottom one corresponds to  $E_2^*$ . H denotes Hopf bifurcation, and it shows that two Hopf bifurcations occur at  $b_2^{H1} = 1.721$  and  $b_2^{H1} = 5.655$ .

follows from Theorem 5.4 that  $E_2^{b_2}$  is unstable when it exists. For  $E_1^*(b_2)$ , numerical calculations show that there are two Hopf bifurcations at  $b_2^{H1}$  and  $b_2^{H2}$ , where  $b_2^{H1} \approx 1.721$ ,  $b_2^{H2} \approx 5.655$ , and indicate that  $E_1^*(b_2)$  is stable if  $b_2 < b_2^{H1}$  or  $b_2 > b_2^{H2}$ . By evaluating the first Lyapunov coefficient  $l_1(b_2)$  of system (2) at  $E_1^*(b_2^{H1})$  and  $E_1^*(b_2^{H2})$ , we obtain that

$$l_1(b_2^{H1}) \approx -2.547 < 0, l_1(b_2^{H2}) \approx -10.6198 < 0.$$

These mean that system (2) undergoes a supercritical Hopf bifurcation at  $b_2 = b_2^{H1}$  and  $b_2 = b_2^{H2}$ , i.e., a stable limit cycle bifurcates from the equilibrium via the Hopf bifurcation when  $b_2$  passes through  $b_2^{H1}$  or  $b_2^{H2}$ .

In order to further understand the effect of phytoplankton allelopathy on the nutrient-plankton system, various values of  $b_2$  are chosen to simulate the dynamical behavior of system (2). These behaviors are illustrated in Figure 9. The parameter values used in Figure 9(a)-(g) are  $b_2 = 1.60, 2.50, 5.05, 5.50, 5.64, 5.66, 5.68$ , respectively, and are also denoted by \* in Figure 4 from which we can see the corresponding  $\lambda$  values. In Figure 9(a), it shows that system (2) has a unique positive equilibrium  $E_1^*$ , and we observe that all solutions converge to  $E_1^*$  since  $b_2 = 1.60 < b_1^{H1}$ . In Figure 9(b),  $b_2 = 2.50$  which is greater than  $b_2^{H1}$ . In this case, the system has a unique positive equilibrium  $E_1^*$ . It follows from Figure 9(b) that there exists a stable periodic solution and all solutions converge to the periodic solution. In Figure 9(c),  $b_2 = 5.05$ . In this case,  $b_2$  passes through the point  $b_2 = b_2^{BP}$ , and system (2) has two positive equilibria  $E_1^*$  and  $E_2^*$  which are both unstable. From Figure 9(c) we observe a stable periodic solution, and, depending on the initial conditions, solutions may either converge to the periodic solution or the boundary equilibrium  $E_\partial$ , i.e., system has switch phenomenon. In Figure 9(d),  $b_2 = 5.50$ . In this case, system (2) has also two positive equilibria  $E_1^*$  and  $E_2^*$  which are both unstable, but the dynamical behaviors are quite different to those shown in Figure 9(c). In Figure 9(d), there is no stable periodic solution, and almost all solutions converge to the boundary equilibrium  $E_\partial$ . Interestingly, as  $b_2$  pass through a critical value  $b_2^c \approx 5.65$ , switch phenomenon appears again for system (2). In Figure 9(e) where  $b_2 = 5.64$ , we observe a stable periodic solution, and, depending on the initial conditions, solutions may either converge to the periodic solution or the boundary equilibrium  $E_\partial$ . In Figure 9(f) where  $b_2 = 5.66$ , system (2) has two positive equilibria  $E_1^*, E_2^*$ , and we observe that solutions may either converge to the positive equilibrium  $E_1^*$  or the boundary equilibrium  $E_\partial$  depending on the initial conditions. The fact that switch phenomenon disappears and reappears later may indicate the possibility that there are two homoclinic bifurcations at some  $b_2^{HC1}$  and  $b_2^{HC2}$ , where  $b_2^{HC1} \approx 5.05$ ,  $b_2^{HC2} = 5.65$ . As  $b_2$  continues to increase and passes through the point  $b_2^{LP}$ , system (2) has no positive equilibrium. As shown in Figure 9(g) all solutions are convergent to the boundary equilibrium  $E_\partial$ . From the above simulation results we can see that the phytoplankton allelopathy may lead to a rich variety of dynamics of the nutrient-plankton system.

Finally, we want to mention that we failed to find an example to confirm the existence of zero-Hopf bifurcation. We can prove that system (2) does not undergo the zero-Hopf bifurcation if  $\alpha > 0.5$ , but it is still a question for the case that  $\alpha < 0.5$ . We are also interested in the global dynamics of system (2), but it seems challenging due to the nonlinearity and the complex dynamics of the system. There are many environmental factors which determines the dynamics of the NPZ system, it is still not clear why certain water bodies would have algal blooming while others

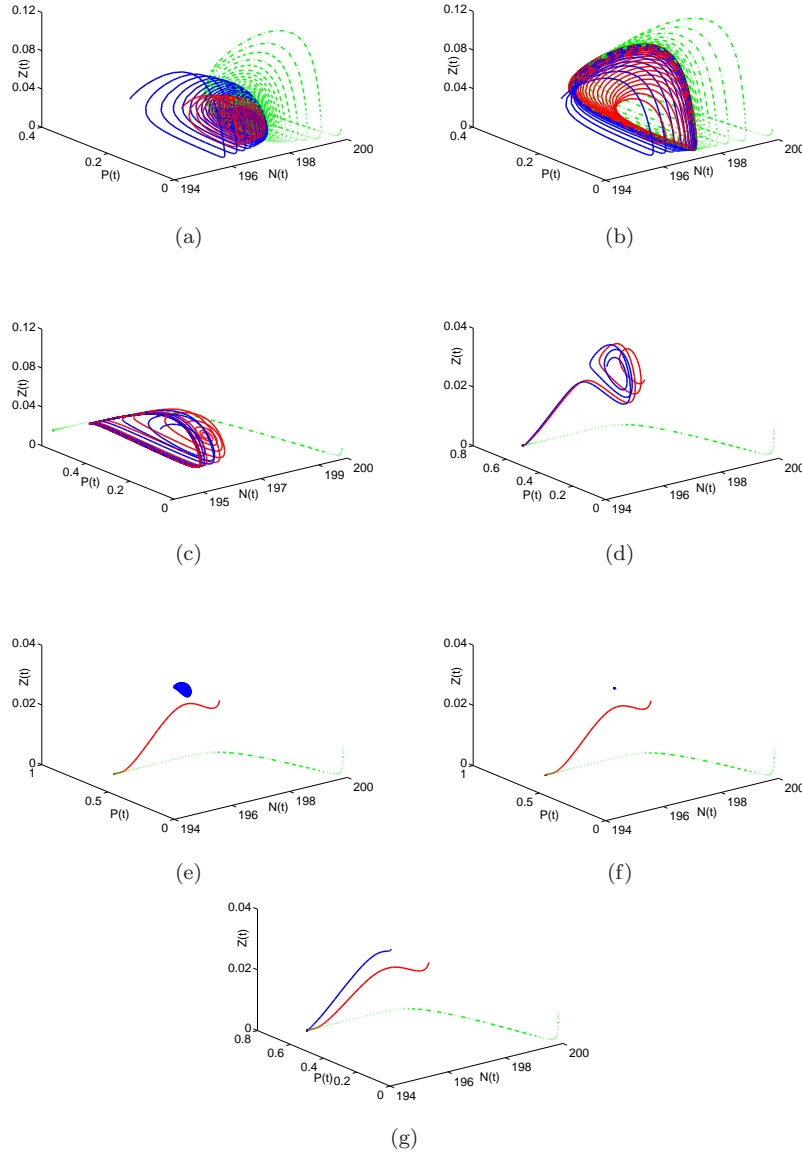


FIGURE 9. Numerical simulations of system (2) for various  $b_2$  values chosen according to the bifurcation diagram in Figure 8 and the value of  $d_1$  is chosen to be  $d_1 = 0.4$ : (a)  $b_2 = 1.60$ ; (b)  $b_2 = 2.50$ ; (c)  $b_2 = 5.05$ ; (d)  $b_2 = 5.50$ ; (e)  $b_2 = 5.64$ ; (f)  $b_2 = 5.66$ ; and (g)  $b_2 = 5.68$ .

do not. By the modeling and analysis of this paper, we defined some major indexes  $\mathcal{R}'_P, \mathcal{R}_P, \mathcal{R}_Z, \mathcal{R}_Z$  which can be used to classify the lakes into different categories. We would expect that each category will have different response when natural environment changes. It will be interesting to use data to verify the classification of freshwater lakes which we keep for future investigation.



**Acknowledgments.** This work was done when the first author Qiu visited Lamps of York University. Qiu would like to thank the helpful discussions with the members of Lamps. Both authors would like to extend their appreciations to the anonymous referee for his/her comments and suggestions that have improved the presentation of this paper.

## REFERENCES

- [1] S. Busenberg, S. K. Kumar, P. Austin and G. Wake, The dynamics of a model of a plankton-nutrient interaction, *Bull. Math. Biol.*, **52** (1990), 677–696.
- [2] J. Chattopadhyay, R. R. Sarker and S. Mandal, Toxin producing plankton may act as a biological control for plankton blooms—field study and mathematical modelling, *J. Theor. Biol.*, **215** (2002), 333–344.
- [3] R. Cropp and J. Norbury, Simple predator-prey interactions control dynamics in a plankton food web model, *Ecol. Model.*, **220** (2009), 1552–1565.
- [4] A. W. Edwards and J. Brindley, Oscillatory behavior in a three-component plankton population model, *Dynam. Stabili. Syst.*, **11** (1996), 347–370.
- [5] A. M. Edwards and J. Brindley, Zooplankton mortality and the dynamical behaviour of plankton population models, *Bull. Math. Biol.*, **61** (1999), 303–339.
- [6] P. G. Falkowski, The role of phytoplankton photosynthesis in global biogeochemical cycles, *Photosynthesis Research*, **39** (1994), 235–258.
- [7] P. J. S. Franks, NPZ models of plankton dynamics: Their construction, coupling to physics, and application, *J. Oceanography*, **58** (2002), 379–387.
- [8] H. I. Freedman and Y. T. Xu, Models of competition in the chemostat with instantaneous and delays nutrient recycling, *J. Math. Biol.*, **31** (1993), 513–527.
- [9] J. P. Grover, D. L. Roelke and B. W. Brooks, Modeling of plankton community dynamics characterized by algal toxicity and allelopathy: A focus on historical *Promnesium parvum* blooms in a Texas reservoir, *Ecological Modelling*, **227** (2012), 147–161.
- [10] J. Hale, *Ordinary Differential Equations*, Krieger, Malabar, 1980.
- [11] B. D. Hassard, N. D. Kazarinoff and Y. H. Wan, *Theory and Application of Hopf Bifurcation*, Cambridge University, Cambridge, 1981.
- [12] S. B. Hsu and P. Waltman, A survey of mathematical models for competition with an inhibitor, *Math. Biosci.*, **187** (2004), 53–91.
- [13] A. Huppert, B. Blasius and L. Stone, A model of phytoplankton blooms, *The American Naturalist*, **159** (2002), 156–171.
- [14] A. Huppert, B. Blasius, R. Olinky and L. Stone, A model for seasonal phytoplankton blooms, *J. Theoret. Biol.*, **236** (2005), 276–290.
- [15] S. E. Jorgenson, A eutrophication model for a lake, *Ecol. Model.*, **2** (1976), 147–165.
- [16] Yu. A. Kuznetsov, *Elements of Applied Bifurcation Theory*, 2<sup>nd</sup> edition, Springer-Verlag, New York, 1998.
- [17] C. Lalli and T. Parsons, *Biological Oceanography: An Introduction*, Butterworth-Heinemann, 1993.
- [18] J. LaSalle and S. Lefschetz, *Stability by Liapunov's Direct Method*, Academic Press, New York, 1961.
- [19] W. M. Liu, Crition of Hopf bifurcations without using eigenvalues, *J. Math. Anal. Appl.*, **182** (1994), 250–256.
- [20] A. Mukhopadhyay, J. Chattopadhyay and P. K. Tapaswi, A delay differential equations of plankton allelopathy, *Math. Biosci.*, **149** (1998), 167–189.
- [21] B. Mukhopadhyay and R. Bhattacharyya, Modelling phytoplankton allelopathy in a nutrient-plankton model with spatial heterogeneity, *Ecological Modelling*, **198** (2006), 163–173.
- [22] R. Pal, D. Basu and M. Banerjee, Modeling of phytoplankton allelopathy with Monod-Haldane-type functional response—a mathematical study, *BioSystems*, **95** (2009), 243–253.
- [23] J. Jiang, Z. Qiu, J. Wu and H. Zhu, Threshold conditions for West Nile virus outbreaks, *Bull. Math. Biol.*, **71** (2009), 627–647.
- [24] G. A. Riley, H. Stommel and D. P. Burrrpus, Qualitative ecology of the plankton of the Western North Atlantic, *Bull. Bingh. Ocean. Coll.*, **12** (1949), 1–169.
- [25] S. Roy, The coevolution of two phytoplankton species on a single resource: Allelopathy as a pseudo-mixotrophy, *Theoret. Populat. Biol.*, **75** (2009), 68–75.

- [26] S. G. Ruan and X. Z. He, [Global stability in Chemostat-type competition models with nutrient recycling](#), *SIAM J. Appl. Math.*, **58** (1998), 170–192.
- [27] J. B. Shukla, A. K. Misra and P. Chandra, [Modeling and analysis of the algal bloom in a lake caused by discharge of nutrients](#), *Applied Math. Comput.*, **196** (2008), 782–790.
- [28] H. L. Smith and P. Waltman, [Perturbation of a globally stable steady state](#), *Proc. Amer. Math. Soc.*, **127** (1999), 447–453.
- [29] J. Sole, E. Garcia-Ladona, P. Ruardij and M. Estrada, [Modelling allelopathy among marine algae](#), *Ecol. Model.*, **183** (2005), 373–384.
- [30] J. H. Steele and E. W. Henderson, [A simple plankton model](#), *The American Naturalist*, **117** (1981), 676–691.
- [31] H. R. Thieme, [Convergence results and a Poincare-Bendixson trichotomy for asymptotically autonomous differential equations](#), *J. Math. Biol.*, **30** (1992), 755–763.
- [32] H. Wan and H. Zhu, [The backward bifurcation in compartmental models for West Nile virus](#), *Math. Biosci.*, **227** (2010), 20–28.
- [33] W. Wang and X. Zhao, [An epidemic model in a patchy environment](#), *Math. Biosci.*, **190** (2004), 97–112.
- [34] J. S. Wroblewski, J. L. Sarmiento and G. R. Fliel, [An ocean basin scale model of plankton dynamics in the North Atlantic. Solutions for the climatological oceanographic condition in May](#), *Global Biogeochem. Cycles.*, **2** (1988), 199–218.
- [35] T. Yoshizawa, *Stability Theory by Liapunov's Second Method*, The mathematical Society of Japan, Tokyo, 1966.

Received September 2015; revised February 2016.

E-mail address: [smoller\\_1@163.com](mailto:smoller_1@163.com)

E-mail address: [huaiping@yorku.ca](mailto:huaiping@yorku.ca)